

# A combination therapy for androgenic alopecia based on quercetin and zinc/copper dual-doped mesoporous silica nanocomposite microneedle patch

Zhaowenbin Zhang<sup>a,b,c,1</sup>, Wenbo Li<sup>d,1</sup>, Di Chang<sup>a,e</sup>, Ziqin Wei<sup>a,c</sup>, Endian Wang<sup>a,c</sup>, Jing Yu<sup>a,c</sup>, Yuze Xu<sup>a,c</sup>, Yumei Que<sup>b</sup>, Yanxin Chen<sup>b</sup>, Chen Fan<sup>b</sup>, Bing Ma<sup>a,c</sup>, Yanling Zhou<sup>a,c</sup>, Zhiguang Huan<sup>a,c</sup>, Chen Yang<sup>b,\*\*\*</sup>, Feng Guo<sup>d,\*\*</sup>, Jiang Chang<sup>a,b,c,\*</sup>

<sup>a</sup> State Key Laboratory of High-Performance Ceramics and Superfine Microstructure, Shanghai Institute of Ceramics, Chinese Academy of Sciences, Shanghai, 200050, PR China

<sup>b</sup> Wenzhou Institute, University of Chinese Academy of Sciences, Zhejiang, 325000, PR China

<sup>c</sup> Center of Materials Science and Optoelectronics Engineering, University of Chinese Academy of Sciences, Beijing, 100049, PR China

<sup>d</sup> Department of Plastic Surgery, Shanghai Jiaotong University Affiliated Sixth People's Hospital, Shanghai, 200025, PR China

<sup>e</sup> Fudan University, Shanghai, 200433, PR China

## ARTICLE INFO

### Keywords:

Microneedle  
Zn<sup>2+</sup> and Cu<sup>2+</sup> dual-doping  
Nanocomposites  
Quercetin  
Androgenic alopecia

## ABSTRACT

A nanocomposite microneedle (ZCQ/MN) patch containing copper/zinc dual-doped mesoporous silica nanoparticles loaded with quercetin (ZCQ) was developed as a combination therapy for androgenic alopecia (AGA). The degradable microneedle gradually dissolves after penetration into the skin and releases the ZCQ nanoparticles. ZCQ nanoparticles release quercetin (Qu), copper (Cu<sup>2+</sup>) and zinc ions (Zn<sup>2+</sup>) subcutaneously to synergistically promote hair follicle regeneration. The mechanism of promoting hair follicle regeneration mainly includes the regulation of the main pathophysiological phenomena of AGA such as inhibition of dihydrotestosterone, inhibition of inflammation, promotion of angiogenesis and activation of hair follicle stem cells by the combination of Cu<sup>2+</sup> and Zn<sup>2+</sup> ions and Qu. This study demonstrates that the systematic intervention targeting different pathophysiological links of AGA by the combination of organic drug and bioactive metal ions is an effective treatment strategy for hair loss, which provides a theoretical basis for development of biomaterial based anti-hair loss therapy.

## 1. Introduction

Hair is an important part of integumentary system. Although the issue of hair loss normally does not endanger human life, it may cause a negative impact on patients' mental health [1]. As one of the most common reasons for hair loss, androgenic alopecia (AGA) affects up to 53% of men and 30% of women in the course of their lives [2–5]. Minoxidil (a vasodilator medication) and finasteride (an androgen inhibitor) are the most commonly used drugs for the treatment of AGA.

However, both of them have certain limitations. For example, minoxidil may cause skin irritation such as itching and stinging, while finasteride may cause erectile dysfunction in men with long-term use [6,7]. Therefore, there is an urgent need to develop new therapies that can efficiently promote hair regeneration with both good effectiveness and biocompatibility. To achieve this goal, the pathogenesis of AGA must be considered. Actually, AGA has been verified as a chronic disease, and the hair follicles under the scalp experience a variety of different stimuli throughout its pathophysiological process [8]. Typically, the

Peer review under responsibility of KeAi Communications Co., Ltd.

\* Corresponding author. State Key Laboratory of High-Performance Ceramics and Superfine Microstructure, Shanghai Institute of Ceramics, Chinese Academy of Sciences, Shanghai, 200050, PR China.

\*\* Corresponding author.

\*\*\* Corresponding author.

E-mail addresses: [cryangchen@ucas.ac.cn](mailto:cryangchen@ucas.ac.cn) (C. Yang), [guofengburn@aliyun.com](mailto:guofengburn@aliyun.com) (F. Guo), [jchang@mail.sic.ac.cn](mailto:jchang@mail.sic.ac.cn) (J. Chang).

<sup>1</sup> Zhaowenbin Zhang, and Wenbo Li contributed equally to this work.

<https://doi.org/10.1016/j.bioactmat.2022.12.007>

Received 20 September 2022; Received in revised form 23 November 2022; Accepted 8 December 2022

2452-199X/© 2022 The Authors. Publishing services by Elsevier B.V. on behalf of KeAi Communications Co. Ltd. This is an open access article under the CC BY-NC-ND license (<http://creativecommons.org/licenses/by-nc-nd/4.0/>).

overexpressed androgen triggers the body to produce large amounts of dihydrotestosterone (DHT), which attacks hair follicles and makes them gradually shrink [8]. When the hair follicle is attacked, a large number of activated immune cells, such as macrophages, T cells, etc. will gather on the scalp, secrete inflammatory factors, and further attack the shrinking hair follicles [9–11]. Meantime, the stem cells in hair follicles surrounding the attacked area are also suppressed away from anagen due to the abnormal microenvironment such as excessive inflammation and injured micro vessels. The sustained attack and delayed repair ultimately lead to the necrosis of hair follicles and the spread of alopecia [11–13]. So, AGA is a systemic disease caused by a variety of factors, mainly including excessive androgen attack, sustained inflammatory response, and lack of active hair follicle stem cells for hair regeneration. Therefore, different from most one-target drug development strategies for AGA treatment, we think therapies to intervene in the above three main pathophysiological links simultaneously may have a better effect on promoting hair regeneration.

Trace elements play an important role in normal hair follicle development and immune cell regulation [14]. For example,  $Zn^{2+}$  is one of the most important essential elements in hair follicles [14,15]. Previous

studies have found that  $Zn^{2+}$  can interact with various biological enzymes (e.g., alkaline phosphatase, dopachrome tautomerase) and regulate the viability of stem cells in hair follicles [16]. Also,  $Zn^{2+}$  acts as a commonly used anti-inflammatory agent since it takes a crucial part in the antioxidant defense system, and it has been reported to induce and maintain an anti-inflammatory microenvironment after being administered for different tissue repairs including skin [17]. Apart from  $Zn^{2+}$ ,  $Cu^{2+}$  also plays a vital role in hair follicles as it can be combined with the human tri-peptide glycyl-L-histidyl-L-lysine in the hair follicles, and further increase the size of the hair follicle, thereby inhibiting hair loss [18–20]. Furthermore,  $Cu^{2+}$  can promote blood vessel formation in skin wounds by up-regulating the angiogenic factors such as vascular endothelial growth factor (VEGF) and hypoxia-inducible factor-1 $\alpha$  (HIF-1 $\alpha$ ), which may benefit the regeneration of hair follicles [21]. More importantly, both  $Zn^{2+}$  and  $Cu^{2+}$  can inhibit 5 $\alpha$ -reductase (the main active enzyme for the conversion of testosterone to DHT) and protect hair follicles [22,23]. However, even though  $Zn^{2+}$  and  $Cu^{2+}$  have many potential benefits for hair follicles, no studies have shown that they have a direct therapeutic effect on AGA so far possibly because of the fact that the metal ions alone are not biologically active enough to achieve

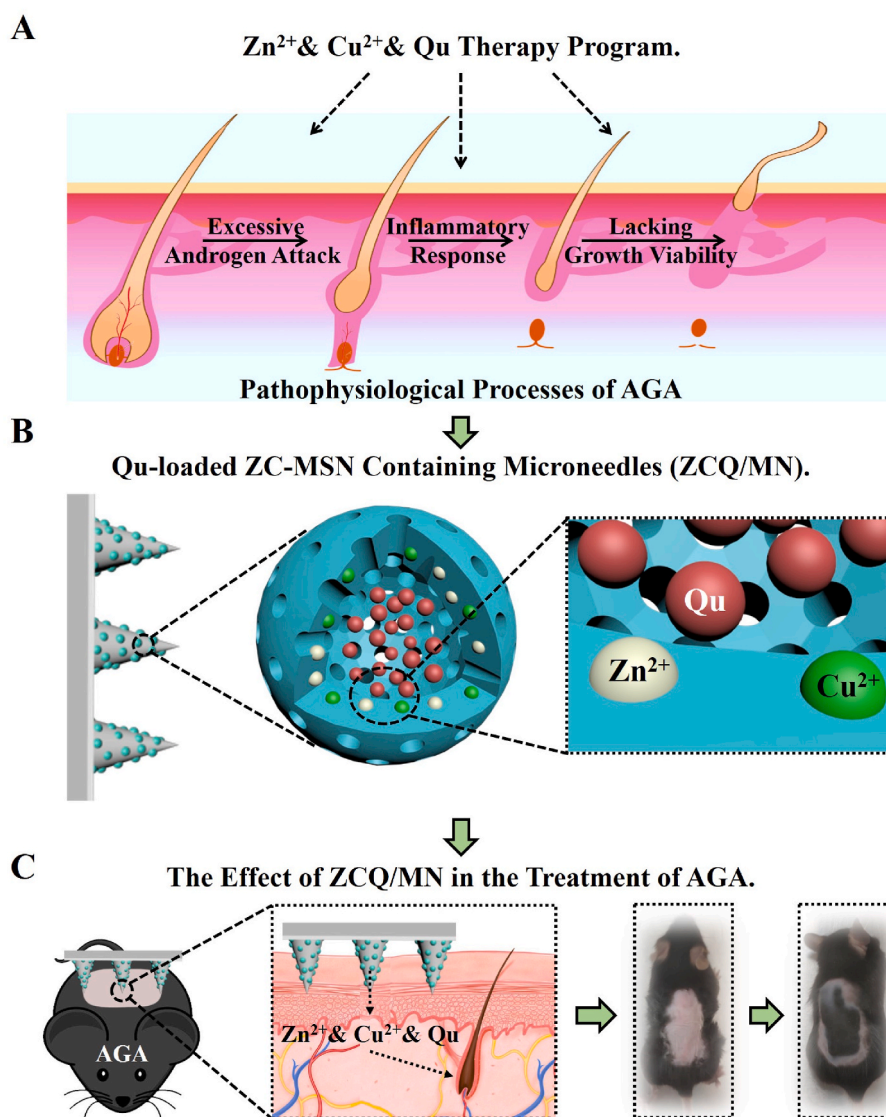


**Fig. 1.** Schematic illustration of ZCQ/MN for AGA. (A)  $Zn^{2+}$  and  $Cu^{2+}$  and Quercetin (Qu) can systematically regulate the pathophysiological microenvironment of hair follicles in patients with AGA. (B) A composite microneedle patch containing Zn/Cu dual-doped mesoporous silica nanoparticles loading with Qu (ZCQ/MN) are designed. (C) ZCQ/MN can release bioactive  $Zn^{2+}$ ,  $Cu^{2+}$  and Qu to treat AGA.

adequate therapeutic effect.

Flavonoids are a class of natural extracts with unique biological functions such as anti-inflammation and promotion of tissue repair [24, 25]. Previous studies have demonstrated that flavonoids such as quercetin (Qu) can interact with different metal ions to form highly bioactive chelates, which further enhance the regeneration of injured tissues as compared with the corresponding pure flavonoids and metal ions alone [25–28]. For example, we have found that the formation of  $\text{Cu}^{2+}$ -Qu chelates accelerates the hair follicle regeneration during burn wound healing [26]. Considering the chelate action of Qu with  $\text{Zn}^{2+}/\text{Cu}^{2+}$  ions, as well as their biological activity on hair follicles, it is possible that the combination of Qu with  $\text{Zn}^{2+}$  and  $\text{Cu}^{2+}$  ions may produce stronger activation for hair follicle regeneration, while the activity for AGA treatment needs to be proved. Therefore, different from one-target approaches in the drug development for AGA treatment, we hypothesize that the synergy of  $\text{Zn}^{2+}$  and  $\text{Cu}^{2+}$  may protect hair follicles by targeting the three main pathophysiological process of AGA such as suppressing the production of DHT, reducing inflammation, and activating hair follicle stem cells, and the interaction between Qu and these two metal ions may further enhance the bioactivity for the treatment of AGA (Fig. 1A). First,  $\text{Zn}^{2+}$  and  $\text{Cu}^{2+}$  may synergistically inhibit DHT, and this effect may be further enhanced by Qu. Secondly,  $\text{Zn}^{2+}$  and Qu may establish an anti-inflammatory microenvironment to alleviate the inflammatory response, and further reduce hair follicle damage. Finally,  $\text{Cu}^{2+}$  and  $\text{Zn}^{2+}$  may synergize with Qu to activate the hair follicle stem cells around the hair loss areas to enhance hair follicle regeneration after AGA.

However, how to deliver the combination of  $\text{Zn}^{2+}$ ,  $\text{Cu}^{2+}$  and Qu to the dermal region of the skin through a rational route of administration is one of the cores to maximize the therapeutic effect of drugs. In terms of skin administration, sustained delivery of drugs in the dermal layer of the skin is a challenge. Direct application of ointment is the most commonly used form of administration at present, but only a few drugs can effectively penetrate into the dermal layer with therapeutic concentrations through this route [29]. Nanoparticles made of biocompatible substance may be effective drug delivery carriers for treating AGA. Minoxidil or finasteride have been incorporated in liposomes nanovesicles and mesoporous silica nanoparticles (MSN) for the treatment of AGA [30–32]. In particular, MSN have been extensively studied for drug delivery. However, due to its stable structure, it has poor degradation performance and low biological activity [33]. In addition, due to the poor solubility of Qu in water, it cannot be fully dissolved in the dermis even loaded in normal MSN or other nanoparticles [34,35], so traditional nano-delivery of Qu may not significantly increase the therapeutic effect on AGA [36]. Interestingly, in our previous work, we have found that single metal element doping can significantly improve the degradation performance of MSN, and the chelation interaction between metal ions and flavonoids can also greatly improve the solubility of flavonoids [26,27]. Therefore, we speculate that two different metal elements such as Zn and Cu may be doped into mesoporous silica for dual ion delivery, and the delivery of quercetin-loaded Zn/Cu dual-doped mesoporous silica nanoparticles to the dermal region of the skin through microneedles can theoretically enable the active ingredients to exert long-term therapeutic effects in the dermal layer of the skin. To proof our hypothesis, in this study, we designed a dissolving microneedle containing mesoporous silica nanoparticles which were dual-doped with  $\text{Zn}^{2+}$  and  $\text{Cu}^{2+}$  and loaded with Qu (ZCQ/MN) for sustained delivery of  $\text{Zn}^{2+}$ ,  $\text{Cu}^{2+}$  and Qu subcutaneously (Fig. 1B and C). We firstly evaluated the therapeutic effects of ZCQ/MN on hair growth in an AGA mouse model. Then, the synergistic effect of the combination of  $\text{Zn}^{2+}$ ,  $\text{Cu}^{2+}$  and Qu in inhibiting androgen damage, alleviating inflammation, and activating hair follicle stem cells and hair regeneration as well as the related mechanisms were studied through *in vitro* cell experiments and *in vivo* burn model experiments.

## 2. Materials and methods

### 2.1. Materials

Sodium hyaluronate (CAS: 9004-61-9), gelatin (CAS: 9000-70-8), sodium alginate (CAS: 9005-38-3), tetraethyl orthosilicate (TEOS, CAS: 78-10-4), copper nitrate trihydrate ( $\text{Cu}(\text{NO}_3)_2 \cdot 3\text{H}_2\text{O}$ , CAS: 10031-43-3), zinc nitrate hexahydrate ( $\text{Zn}(\text{NO}_3)_2 \cdot 6\text{H}_2\text{O}$ , CAS: 10196-18-6), ammonium fluoride ( $\text{NH}_4\text{F}$ , CAS: 12125-01-8), cetyltrimethylammonium bromide (CTAB, CAS: 57-09-0), zinc chloride ( $\text{ZnCl}_2$ , CAS: 7646-85-7), copper chloride ( $\text{CuCl}_2$ , CAS: 10125-13-0), and sodium silicate ( $\text{Na}_2\text{SiO}_3$ , CAS: 13517-24-3) were purchased from Sinopharm Chemical Reagent Co., Ltd (Shanghai, China). Quercetin (CAS: 117-39-5) was purchased from Adamas (Product Code: 16042C).

### 2.2. Preparation of zinc/copper dual-doped mesoporous silica nanoparticles (ZC-MSN)

The sol-gel method was used to prepare ZC-MSN. First, 1.82 g of CTAB and 3.00 g of  $\text{NH}_4\text{F}$  were added to a beaker containing 500 mL of deionized water and stirred at 80 °C for 1 h. Then, 2.43g of  $\text{Cu}(\text{NO}_3)_2 \cdot 3\text{H}_2\text{O}$  and 2.66g of  $\text{Zn}(\text{NO}_3)_2 \cdot 6\text{H}_2\text{O}$  were dissolved in above reaction solution and stirred for 1 h. Next, 9 mL of TEOS was dropped into the above reaction solution. After 4 h of reaction, the beaker was taken out from the 80 °C water bath, cooled to room temperature. The above solution was centrifuged at 8000 rpm for 25 min, and then washed alternately with absolute ethanol and deionized water. Finally, the powder obtained by freeze-drying the washed sample was calcined in a muffle furnace at 600 °C for 6 h to obtain ZC-MSN. Pure MSN, Cu doped MSN (Cu-MSN) and Zn doped MSN (Zn-MSN) were also synthesized as control groups by the same procedure using the corresponding ingredients with the same amounts.

### 2.3. Preparation of quercetin loaded nanoparticles

Briefly, 0.2 g of nanoparticles (MSN, Zn-MSN, Cu-MSN, and ZC-MSN) were dispersed into 100 mL alcohol solution containing quercetin (Qu, 2 mg/mL). The mixed solution was fully stirred for 48 h, and then centrifuged at 8000 rpm for 5 min. The sediment was washed with alcohol three times to remove the quercetin on the surface of the nanoparticles, and then freeze-dried for 24 h to obtain Qu loaded nanoparticles.

### 2.4. Preparation of quercetin-loaded ZC-MSN composite dissolving microneedle (ZCQ/MN)

ZCQ/MN was fabricated based on a polydimethylsiloxane (PDMS) mold (Microneedle array: 20\*20). Briefly, 2g of sodium hyaluronate, 0.5g of gelatin and 2.5g of sodium alginate were dissolved in 50 mL deionized water at 45 °C. The reason for choosing these three polymers for microneedles preparation is to obtain microneedles with good biocompatibility, appropriate dissolution rate and mechanical strength [37–39]. Then, 0.5g of ZCQ nanoparticles, ZC nanoparticles or Qu powders was added to the above solution and the mixed solution was continuously stirred for 24 h. Next, 1 mL of the solution was dropped on the PDMS mold and then transferred to a vacuum drying oven (45 °C) for 2 h. Finally, the mold was transferred to an oven (45 °C) and placed for 72 h to for demolding. The pure microneedles (MN), Qu loaded microneedles (Qu/MN) and ZC-MSN loaded microneedles (ZC/MN) were also prepared as control groups follow the same protocol using the corresponding ingredients with the same amounts.

### 2.5. Characterization of nanoparticles and microneedles

The surface morphology of ZC-MSN and was observed using scanning electron microscope (SEM, S-4800, Hitachi, Japan) and

transmission electron microscope (TEM, JEM-2100F, JEOL, Japan), while the element content (O, Si, Cu, Zn) in ZC Nanoparticles was detected by SEM accessory energy-dispersive spectrometer (EDS) system. The optical images of different microneedles were taken by a camera, and their surface morphologies were observed using SEM. The dissolution performance of different microneedles was evaluated by putting a rectangular piece of microneedles ( $1 \times 2 \text{ cm}^2$ ) in 10 mL of deionized water at  $25^\circ\text{C}$  for 24 h, and the optical photos at 0, 4, 12 and 24 h were taken for observation. The ion ( $\text{Zn}^{2+}$ ,  $\text{Cu}^{2+}$  and  $\text{SiO}_3^{2-}$ ) release concentration was measured using an inductively coupled plasma-atomic emission spectrometry (ICP-AES, Thermo Fisher X Series 2, USA).

## 2.6. Quercetin releasing profile from ZC-MSN and ZCQ/MN

For ZC-MSN, 10 mg of Qu loaded nanoparticles were added into 1 mL of phosphate buffered solution (PBS) for different times (1, 3, 5, 7, and 14 days), and then the suspension was collected by centrifugation (8000 rpm, 5 min), respectively. The release concentration was measured using an ultraviolet–visible (UV/Vis) spectrophotometer at 374 nm. For ZCQ/MN, a square piece of ZCQ/MN ( $1 \times 1 \text{ cm}^2$ ) was put into PBS buffer at  $37^\circ\text{C}$  for 24 h (ZC/MN and Qu/MN were used as the control group). Then, the above solution was centrifuged at 8000 rpm for 5 min and the supernatant was collected. The collected release medium was analyzed to determine the Qu concentration by the UV/Vis spectroscopy.

## 2.7. The compressive and penetration test of ZCQ/MN on mouse skin

8-week-old C57BL/6 mice were purchased from Chinese Academy of Science Shanghai Laboratory Animal Center (SLACAS). The mice were randomly divided into 2 groups (Blank group and ZCQ/MN group). First, the hair on the dorsal skin was removed by shaving an area of  $2 \times 3 \text{ cm}^2$ . Then, ZCQ/MN was pressed into the back of the mice. Mice were killed and the skins were obtained for H&E staining to observe the compression and penetration of microneedles.

## 2.8. Androgenic alopecia (AGA) model establishment, treatment and performance evaluation

8-week-old C57BL/6 mice were purchased from Chinese Academy of Science Shanghai Laboratory Animal Center (SLACAS). All animal operations were performed in accordance with the guidelines for the care and use of laboratory animals in Shanghai Jiao Tong University (Shanghai, China), and approved by the Animal Ethics Committee of the Sixth People's Hospital Affiliated to Shanghai Jiao Tong University School of Medicine (Shanghai, China). Firstly, testosterone solution was injected subcutaneously under the dorsal skin of C57BL/6 mice to induce the AGA model. Each animal was injected daily with 0.1 mL of 5 mg/mL of testosterone solution throughout the experimental period (28 days). On day 14 post-injection, the hair on the dorsal skin was removed by shaving an area of  $2 \times 3 \text{ cm}^2$ . The mice were randomly divided into 5 groups ( $n = 6$ ) as follows: Blank group, MN group, Qu/MN group, ZC/MN group and ZCQ/MN group. The skin of each animal was photographed every 4 days. In addition, healthy mice without testosterone injection were used as positive control group. The skin color changed from pink to black indicates anagen initiation [40]. At the end of the experiment, the area with new hair covering in the treated skin was measured, and the skin of each animal was harvested for subsequent studies. Tissue samples were fixed in 4% paraformaldehyde for 48 h. After paraffin embedding, the tissue samples were cut into  $7 \mu\text{m}$  sections and processed according to our previous work [16]. Briefly, the sections were stained using hematoxylin and eosin (H&E, Sigma-Aldrich) for histological analysis according to the manufacturer's instructions. After that, the primary antibody solution containing cyokeratin 19 (sc-376126, Santa Cruz) and CD68 (PA5-89134, ThermoFisher) were used for immunostaining. The tissue specimens were examined by

microscopy for the analysis of hair follicle formation.

## 2.9. Cell culture

Human umbilical vein endothelial cells (HUVECs) were cultured in the endothelial cell culture medium (ECM) (Sciencell, USA) containing 5% (v/v) fetal bovine serum (FBS, Thermo Trace Ltd., Melbourne, Australia) and 1% (v/v) endothelial cell growth supplement/heparin kit (ECGS/H, Promocell). Human hair follicle dermal papilla cells (HHDPCs) were cultured in a mesenchymal stem cell culture medium (MSCM) (Sciencell, USA) containing 5% (v/v) fetal bovine serum (FBS, Thermo Trace Ltd., Melbourne, Australia) and 1% (v/v) mesenchymal stem cell growth supplement (MSCGS). Macrophages (Raw264.7) were cultured in the DMEM containing 10% (v/v) fetal bovine serum (FBS, Thermo Trace Ltd., Melbourne, Australia). In this study, all cells used were between passages 7 and 10.

## 2.10. Preparation of cell culture media containing $\text{Zn}^{2+}$ , $\text{Cu}^{2+}$ , $\text{SiO}_3^{2-}$ , Qu or their combinations

Cell experiments were performed using the media containing a certain concentration of  $\text{Zn}^{2+}$ ,  $\text{Cu}^{2+}$ ,  $\text{SiO}_3^{2-}$ , Qu or their combinations, which were prepared by adding the corresponding amount of zinc chloride, copper chloride, sodium silicate, Qu or their combinations in normal cell culture media, respectively. The concentrations of  $\text{Zn}^{2+}$ ,  $\text{Cu}^{2+}$ ,  $\text{SiO}_3^{2-}$ , Qu were determined based on the preliminary experiments as the effects of different concentrations of  $\text{Zn}^{2+}$ ,  $\text{Cu}^{2+}$ ,  $\text{SiO}_3^{2-}$ , or Qu on HHDPCs viability were evaluated. Briefly, cells ( $1 \times 10^3$  cells per well) were seeded on 96-well culture plates. After incubating for 24 h, the cell culture media was changed with media containing different concentrations of  $\text{Zn}^{2+}$ ,  $\text{Cu}^{2+}$ ,  $\text{SiO}_3^{2-}$ , or Qu and then cultured for another 24 h. The cell viability was measured by absorbance of all samples at 450 nm in a microplate reader (SpectraMax, Plus 384, Molecular Devices, Inc., USA) under CCK-8 (Cell Counting Kit-8, Dojindo, Kumamoto, Japan) reagent. The optimal concentration of  $\text{Zn}^{2+}$ ,  $\text{Cu}^{2+}$ ,  $\text{SiO}_3^{2-}$ , or Qu was chosen for further study.

## 2.11. The synergistic effect of $\text{Zn}^{2+}$ , $\text{Cu}^{2+}$ , and Qu (ZCQ) on cell proliferation and migration

For cell proliferation, the viability of HUVECs, HHDPCs and Raw264.7 under the treatment of  $\text{Zn}^{2+}$ ,  $\text{Cu}^{2+}$ , Qu or their combinations for different times (1, 3, and 5 days) were conducted followed the same procedure as above. For cell migration, cells (HUVECs, HHDPCs and Raw264.7) were first seeded in six-well plates and cultured up to about 80% confluency, followed by serum-free starvation over 24 h to reset the cell cycle. Then, the cell monolayer in each well was scrapped with a plastic tip (200  $\mu\text{L}$ ) and washed with PBS (0 h). Meanwhile, the cell culture media were changed to media containing  $\text{Zn}^{2+}$ ,  $\text{Cu}^{2+}$ , Qu or their combinations. The optical images were obtained at 0, 12h and 24 h using an optical microscope (Leica, Germany). The cells were stained with crystal violet (CV) for 1 min, and optical images were obtained using the above optical microscope. The migration rate was analyzed using ImageJ software (National Institutes of Health, USA) and determined by the ratio of the initial scratch area and the final scratch area.

## 2.12. The synergistic effect of ZCQ on protecting HHDPCs injured by dihydrotestosterone (DHT)

DHT was used to induce cell injured model similar to the previous study [41]. Briefly, HHDPCs ( $1 \times 10^3$  cells per well) were seeded on 96-well culture plates. After 24 h, the cell culture media were replaced with a mixed solution containing DHT (5 nmol/mL), and  $\text{Zn}^{2+}$ ,  $\text{Cu}^{2+}$ ,  $\text{SiO}_3^{2-}$ , Qu or their combinations. for 48 h. The normal cell culture medium was used as control. The cell viabilities in different groups were detected as above. Meanwhile, cells were also fixed with 4% paraformaldehyde

solution and stained with crystal violet (CV) for 1 min, and optical images were obtained using the above optical microscope.

### 2.13. Sequencing

RNA sequencing was performed by Shanghai Weiao Biological Technology Co., Ltd. Briefly, HHDPs ( $1 \times 10^5$  cells per well) were seeded on 6-well culture plates. The cells were treated with the above-mentioned media for 72 h. Then, HHDPs were washed twice with preheated PBS and the total RNA was extracted from cells using Trizol reagent (Invitrogen, USA). The concentrations of total RNA were assayed by a nanodrop 2000 reader (Thermo Scientific, USA). Then, cDNA was synthesized using a Prime-Script™ RT reagent kit (Takara Bio, Shiga, Japan) according to the manufacturer's recommendations. cDNA was then sequenced on an Illumina HiSeq X-Ten (LC Bio, China). FastQC v.0.11.4 software was used to evaluate the raw data and obtain the clean reads. The reads were mapped to the human genome GRCz11 using HISAT2 as a previously published method [42]. Gene expression was quantified by calculating the reads per kilobase transcriptome per million mapped reads (RPKM). Genes with fold change  $>1$  and false discovery rate (FDR)  $< 0.05$  were considered as a significant difference.

### 2.14. The gene expression in normal or injured HHDPs treated by ZCQ

Gene expression of PDGF, TGF- $\beta$ , C-Myc, MMP2 and CCN1 in normal or injured HHDPs were detected by quantitative PCR (qPCR). Briefly, HHDPs ( $1 \times 10^5$  cells per well) were seeded on 6-well culture plates. The cells were treated with the above-mentioned media for 72 h. Then, HHDPs were washed twice with preheated PBS and the total RNA was extracted from cells using Trizol reagent (Invitrogen, USA). The concentrations of total RNA were assayed by a nanodrop 2000 reader (Thermo Scientific, USA). Then, cDNA was synthesized using a Prime-Script™ RT reagent kit (Takara Bio, Shiga, Japan) according to the manufacturer's recommendations. Primers for the stem cell markers containing PDGF, TGF- $\beta$ , C-Myc, MMP2 and CCN1 and the housekeeping gene GAPDH were synthesized commercially (Shengong, Co. Ltd. Shanghai, China). Quantification of all cDNA of stemness marker genes was performed with Bio-Rad MyiQ single color Real-time PCR system. All experiments were done in triplicate to obtain the average data. The sequences of primers were as follows: PDGF (5'-GAA TCA TAG CTC TCT CCT CGC AC-3' and 5'-GAT TCC TCC AAA GCC TCA TAG CAG-3'), C-Myc (5'-AAT AGA GCT GCT TCG CCT AGA-3' and 5'-GAG GTG GTT CAT ACT GAG CAA G-3'), TGF- $\beta$  (5'-ACC TTG GGC ACT GTT GAA GT-3' and 5'-CTC TGG GCT TGT TTC CTC AC-3'), MMP2 (5'-ACA GCA GGT CTC AGC CTC AT-3' and 5'-TGA AGC CAA GCG GTC TAA GT-3'), CCN1 (5'-CTC CCT GTT TTT GGA ATG GA-3' and 5'-TGG TCT TGC TGC ATT TCT TG-3') and GAPDH (5'-TGG CAA ATT CCA TGC AC-3' and 5'-CCA TGG TGG TGA AGA CGC-3').

### 2.15. The synergistic effect ZCQ on reducing the expression of inflammatory factors in Raw264.7

Gene expression of TNF- $\alpha$  and IL-6 in Raw264.7 with different treatments were detected by qPCR following the above protocol. The sequences of primers were as follows: TNF- $\alpha$  (5'-CTG TAG CCC ACG TCG TAG CAA-3' and 5'-TGT CTT TGA GAT CCA TGC CGT T-3'), IL-6 (5'-ATA GTC CTT CCT ACC CCA ATT TCC-3' and 5'-GAT GAA TTG GAT GGT CTT GGT CC-3'), and GAPDH (5'-AGA ACA TCA TCC CTG CAT CCA C-3' and 5'-TCA GAT CCA CGA CGG ACA CA-3')

### 2.16. The synergistic effect of ZCQ on protecting inflammatory injured HHDPs

Raw 264.7 ( $5 \times 10^5$  cells per well) was seeded in Transwell chambers of 6-well culture plates and pre-incubated with 1  $\mu\text{g}/\text{mL}$  lipopolysaccharide (LPS) for 24 h. Meanwhile, HHDPs ( $1 \times 10^5$  cells per well)

were seeded in 6-well culture plates and pre-cultured with normal medium for 24 h. The Transwell chambers seeded with Raw 264.7 were then transferred to 6-well plates seeded with HHDPs, and the culture media was all replaced with media containing  $\text{Zn}^{2+}$ ,  $\text{Cu}^{2+}$ , Qu or their combination. After culturing for 72 h, the cells were stained with live/dead cell dyes (Calcein AM and ethidium homodimer-1) to label live cells with green fluorescence and dead cells with red fluorescence, respectively. The state of the cells was observed by a confocal laser scanning microscope (Leica TCS SP8, Germany).

### 2.17. Deep third degree burn wound model establishment, treatment and performance evaluation

8-week-old Sprague Dawley (SD) female rats (220g) were purchased from CAS Shanghai Laboratory Animal Center (SLACAS). All animal operations were performed in accordance with the guidelines for the care and use of laboratory animals in Shanghai Jiao Tong University (Shanghai, China), and approved by the Animal Ethics Committee of the Sixth People's Hospital Affiliated to Shanghai Jiao Tong University School of Medicine (Shanghai, China). A total of 30 rats were used in this study and lived in the Laboratory Animal Center of the Sixth People's Hospital of Shanghai Jiao Tong University School of Medicine in a pathogen-free environment. In order to test the actual application ability of ZCQ/MN, we modified the previous scheme to prepare a full-thickness third-degree burn wound model [26]. The rats were randomly divided into 5 groups ( $n = 6$ ) as follows: Blank group, MN group, Qu/MN group, ZC/MN group and ZCQ/MN group. The skin of each animal was harvested for subsequent studies.

Tissue samples were obtained on day 10 and day 24 and fixed with 4% paraformaldehyde. After 48 h, the tissue samples were embedded in paraffin and cut into 7  $\mu\text{m}$  thickness. Subsequently, the slices were subjected to H&E staining histochemical analysis. After that, the primary antibody solution containing cytokeratin 19 (sc-376126, Santa Cruz), or rabbit anti-CD31 (ab9498, Abcam) was used for immunostaining. The number of new hair follicles on 24th day was determined by counting three randomly selected image areas according to the cytokeratin 19 staining. The number of new blood vessels on 24th day was determined by counting three randomly selected image areas according to the CD31 staining.

### 2.18. Wound healing rate

Photographs of the wound area were taken until the 24th day. The size of the wound area at different time points was determined by ImageJ (National Institutes of Health, USA). By measuring the area of the initial wound and the wound area at the corresponding time point, the wound healing rate ((area at the corresponding time point)/initial area  $\times 100\%$ ) is calculated.

### 2.19. Statistical analysis

All results were expressed as means  $\pm$  standard deviation. Multiple comparisons between groups were performed using one-way ANOVA testing with a post hoc test. Statistical significance was considered when  $*P < 0.05$  or  $**P < 0.01$  or  $***P < 0.001$ .

## 3. Results

### 3.1. The characterization of nanoparticles

Firstly, Zn and Cu dual-doped mesoporous silica nanoparticles (ZC-MSN) with uniform dispersibility and mesoporous channels ( $\sim 50$  nm) were successfully synthesized and characterized by scanning electron microscopy (SEM) and transmission electron microscopy (TEM) revealing uniform particle size and mesopores (Fig. 2A). The content of each element in ZC-MSN was analyzed by energy dispersive

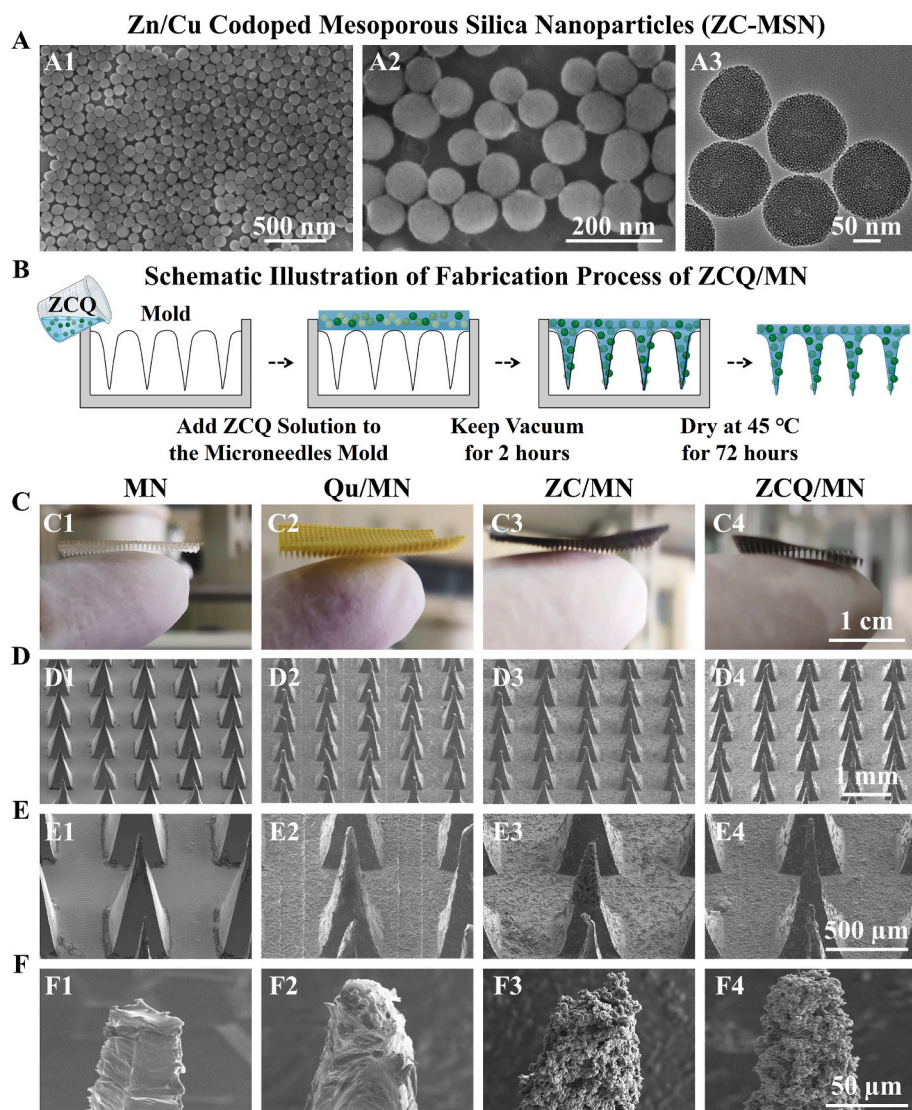


**Fig. 2.** Characterization of nanoparticles and microneedles. (A) The SEM (A1, A2) and TEM (A3) images of zinc and copper dual-doped mesoporous silica nanoparticles (ZC-MSN). (B) The schematic illustration of fabrication process of ZCQ/MN. (C–F) Optical photographs and SEM images of hyaluronic acid/sodium alginate/gelatin microneedles (MN), quercetin microneedles (Qu/MN), ZC-MSN microneedles (ZC/MN) and quercetin-loaded ZC-MSN microneedles (ZCQ/MN). (C1–C4) Optical photographs of microneedles. (D1–D4) SEM images of the microneedle array. (E1–E4) SEM image of a single microneedle. (F1–F4) SEM images of the tip of the microneedle.

spectrometer (EDS), which shows that the mass ratio of Zn, Cu, Si, O were 4.53%, 14.23%, 33.74% and 47.51% respectively (Fig. S1). Furthermore, the ion release behavior of ZC-MSN was evaluated by Inductively Coupled Plasma Emission Spectrometer (ICP). It can be found that there is no significant difference in the concentrations of  $Zn^{2+}$ ,  $Cu^{2+}$  and  $SiO_3^{2-}$  released from dual-ion doped mesoporous silica nanoparticles (ZC-MSN) as compared to single Cu or Zn doped mesoporous silica nanoparticles (Zn-MSN and Cu-MSN) (Fig. S2). The cumulative release of  $Zn^{2+}$ ,  $Cu^{2+}$ , and  $SiO_3^{2-}$  reached 4.87  $\mu\text{g/mL}$ , 5.22  $\mu\text{g/mL}$  and 80.53  $\mu\text{g/mL}$  respectively in 14 days, which was within the biologically active concentration range of the individual ions [26,43,44]. Sequentially, the Qu loading and release property of ZC-MSN were evaluated. One of the challenges with the application of flavonoids such as Qu is the low water solubility and bioavailability. An interesting observation in the present study is that the ZC-MSN loaded significantly more Qu ( $241.17 \pm 5.28 \text{ mg/g}$ ) than MSN ( $81.33 \pm 1.96 \text{ mg/g}$ ). This is probably mainly because of chelation between  $Cu^{2+}$  and Qu since Cu-MSN also increased the loading of Qu ( $237.26 \pm 3.98 \text{ mg/g}$ ), while Zn-doping might not have significant contribution to the loading dose of Qu ( $82.30 \pm 2.05 \text{ mg/g}$ ) as compared to the MSN (Fig. S3). Meanwhile, the higher loading dose of Qu also allowed ZC-MSN to sustainably release more Qu within 14 days (cumulative release concentration: 2.81–6.53  $\mu\text{g/mL}$ ) as compared to MSN and Zn-MSN (Fig. S4).

### 3.2. The characterization of microneedles

In this study, sodium alginate, hyaluronic acid and gelatin were used to prepare microneedles (MN), Qu-loaded microneedles (Quercetin was loaded directly into the microneedle patch.) (Qu/MN), ZC-MSN containing microneedles (ZC/MN) and Qu-loaded ZC-MSN containing microneedles (ZCQ/MN). It can be found from the optical photos that the pure polymer microneedle patch without drug loading is transparent, and its color will change with the additives. When Qu was added to the microneedle, the microneedle patch became yellow, and when ZC-MSN or Qu-loaded ZC-MSN was added to the microneedle, the microneedle patch became black (Fig. 2B1–B4). The SEM images showed that the microneedle arrays in all groups were evenly arranged with a tip height of about 600  $\mu\text{m}$  (Fig. 2C1–C4). However, the incorporation of Qu, ZC-MSN or Qu-loaded ZC-MSN obviously increased the surface roughness of the microneedles as shown in higher magnification SEM images (Fig. 2D1–D4), especially for ZC/MN and ZCQ/MN groups, in which the enriched nanoparticles were observed on the needle tips (Fig. 2E3 and E4).

Furthermore, the dissolubility of the microneedles was verified in deionized water at 25 °C for 24 h. The dissolution rate of each group was similar as all microneedles swelled and broke in 12 h, and almost completely dissolved after 24 h (Fig. S5A). In addition, the

concentrations of the released ions and Qu from Qu/MN, ZC/MN, and ZCQ/MN in 24 h were evaluated. As shown in Fig. S5B, more  $\text{Cu}^{2+}$  was released from ZCQ/MN ( $1.73 \pm 0.14$  ppm) than ZC/MN ( $0.41 \pm 0.09$  ppm) group, while no significant differences were shown in the release of  $\text{Zn}^{2+}$  or  $\text{SiO}_3^{2-}$  between these two groups. Also, the same level of Qu was detected in Qu/MN ( $1.45 \pm 0.09$   $\mu\text{g}/\text{mL}$ ) and ZCQ/MN ( $1.57 \pm 0.21$   $\mu\text{g}/\text{mL}$ ) group, indicating the complete release of Qu from ZCQ (Fig. S5C).

In addition, the penetration of ZCQ/MN on mouse skin was also evaluated to ensure that the prepared microneedles can deliver the bioactive substance to the dermis. The result showed that ZCQ/MN could penetrate the dermis about 300  $\mu\text{m}$ , which proved that the mechanical strength of microneedles was suitable for subcutaneous drug delivery (Fig. S8).

### 3.3. Effect of ZCQ/MN on AGA

C57BL/6 mice were used to establish a testosterone-induced AGA model, and then treated with different microneedles (MN, Qu/MN, ZC/MN, and ZCQ/MN). As shown in Fig. 3A, no hairs or hair roots re-growth was observed on the back of the mice in all testosterone-induced groups within the first 6 days after removing hairs from the skin, while the healthy mice already started new hair growth, which proved successful establishment of the AGA model. On day 10, visible hairs were observed in both Qu/MN and ZCQ/MN groups, while only black hair roots were appeared in Blank, NM, ZC/MN groups. It is apparent that, in comparison to Qu/MN group, ZCQ/MN group showed more hair regrowth. On day 14, a few hairs were appeared on the back of the mice in Blank and MN groups. In contrast, significantly more hairs were shown in Qu/MN and ZCQ/MN groups, and it is clear to see that the ZCQ/MN group had the best hair growth as the back of mice in this group was almost fully

covered with new hairs. Correspondingly, the hair coverage rate was counted, and presented in Fig. 3B. The ZCQ/MN group had the best hair coverage rate as compared with Qu/MN and ZC/MN groups, while Qu/MN group had slightly higher hair coverage rate than ZC/MN group. Surprisingly, the hair coverage of the ZCQ/MN group even reached 95.33% on the 14th day, indicating that the newly regenerated hairs almost completely covered the alopecia area. In addition, the area covered by hair on the back of mice on day 14 was also calculated (Fig. 3C), which confirmed the finding that the microneedle with the combination of Qu and ions (ZCQ/MN,  $5.57 \pm 0.35$   $\text{cm}^2$ ) significantly promoted the hair growth in mice after testosterone damage, while single Qu (Qu/MN,  $3.38 \pm 0.06$   $\text{cm}^2$ ) or ion combination (ZC/MN,  $2.09 \pm 0.05$   $\text{cm}^2$ ) also revealed certain therapeutic effect.

Furthermore, histological and immunohistochemical analysis were applied to evaluate the hair regeneration. The hematoxylin-eosin (H&E) and Cytokeratin 19 (CK19) staining displayed that ZC/MN, Qu/MN and ZCQ/MN promoted the formation and growth of hair follicles. It could be clearly observed that almost all hair follicles have grown black hair shafts in the ZCQ/MN and Healthy groups, indicating that the hair follicles in the ZCQ/MN group have becoming matured. In addition, a few hair follicles have grown black hair shafts in the ZC/MN and Qu/MN groups, and hair shafts in the Qu/MN group were significantly larger than that in ZC/MN group. In contrast, the hair follicles in the MN and Blank groups were morphologically still in the primary stage, because the hair follicle stem cells were just starting to aggregate, proliferate and divide in these groups (Fig. 3D and E). This result indicates that Qu may be the key to promote the differentiation and maturation of stem cells. When we compare the Qu/MN and ZCQ/MN groups, it is interesting to see that in Qu/MN group the hair shaft was still in round shape, while in the ZCQ/MN group the hair shaft was already fusiform indicating that the hair follicle tissue was getting mature. This result suggests that,

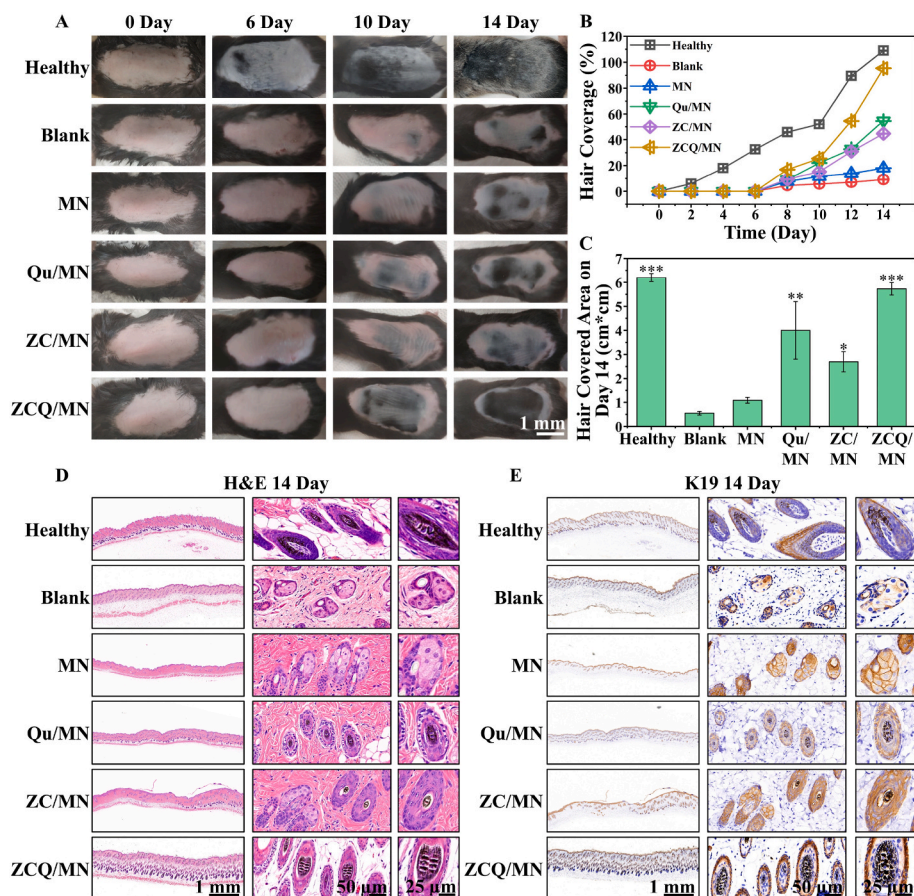


**Fig. 3.** ZCQ/MN promotes hair growth in testosterone-induced AGA mice model. (A) Representative optical images of hair growth on the 0<sup>th</sup>, 6<sup>th</sup>, 10<sup>th</sup>, and 14<sup>th</sup> day after treatment with different microneedles (MN, Qu/MN, ZC/MN, and ZCQ/MN). Blank group was mice treated with medical gauze. Healthy group was mice without testosterone injection. (B) The hair coverage on the back of mice from day 0 to day 14 (n = 3). (C) Hair covered area of dorsal skin of mice after 14-days treatment with different formulations (n = 3). (D) Representative H&E staining images of newborn hair follicles on 14th day. (E) Representative immunohistochemical staining images of cytokeratin 19 indicating newborn hair follicles on 14th day (\*p < 0.05, \*\*p < 0.01, \*\*\*p < 0.001 vs. MN.).

although Qu is highly active to stimulate hair growth, it alone is not strong enough to promote the maturation of the growing hair follicles, and bioactive ions are required for the maturation. The combination of Zn/Cu ions with Qu results in the most effective stimulation of the hair follicle growth and maturation, and therefore achieve the expected therapeutic effect on AGA.

### 3.4. The synergistic protective effect of Zn<sup>2+</sup>, Cu<sup>2+</sup>, and Qu on human hair follicle dermal papilla cells injured by dihydrotestosterone

In order to further explore the roles of different ions and Qu played in the treatment, cell experiments were performed using the media containing a certain concentration of different ions and Qu or their combinations. The concentrations of Zn<sup>2+</sup>, Cu<sup>2+</sup>, SiO<sub>3</sub><sup>2-</sup>, Qu were firstly determined based on the preliminary experiments using different concentrations of Zn<sup>2+</sup>, Cu<sup>2+</sup>, SiO<sub>3</sub><sup>2-</sup>, Qu to treat HHDPs. According to the results, Zn<sup>2+</sup> (1.5 ppm), Cu<sup>2+</sup> (1.5 ppm), SiO<sub>3</sub><sup>2-</sup> (15 ppm), Qu (1.5 μg/mL) were selected for further cell culture experiments (Fig. S6).

Dihydrotestosterone (DHT, 5 nmol/mL) was then used to establish an injured HHDPs model. As shown in Fig. 4A, the purple crystal staining of HHDPs confirmed the successful establishment of injured cell model as DHT significantly decreased the proliferation of HHDPs and altered the cytoskeleton to be atrophic. The treatment of Zn<sup>2+</sup>, Cu<sup>2+</sup> or Qu alone slightly alleviated the DHT-induced cell damage as more HHDPs proliferated with well-spread cell morphology, while the combination of each two of them (ZC, ZQ, CQ) or all three of them (ZCQ) further enhanced the cell protection effect, and the three-component combination of ZCQ showed the best recovery of the cell morphology and viability. The corresponding quantification of cell proliferation was assessed by CCK8 assay kit, and the results are presented in Fig. 4B, which confirmed the conclusion that the ZCQ group showed the best protective effect on HHDPs from DHT attacks and significantly enhanced cell proliferation, while single Zn<sup>2+</sup>, Cu<sup>2+</sup> or Qu also showed gentle protective effect. More interestingly, SiO<sub>3</sub><sup>2-</sup> alone had no inhibitory effect on DHT-induced cell damage, which suggested that the

therapeutic effect of ZCQ was mainly attributed to the combination of Zn<sup>2+</sup>, Cu<sup>2+</sup> and Qu.

Moreover, the RNA sequencing of DHT-injured HHDPs before and after the treatment with ZCQ was analyzed. As shown in Fig. 4C, we found that 722 genes were up-regulated and 1458 genes were down-regulated after the treatment of ZCQ. Among these genes, we identified 5 genes most associated with hair follicle growth phases, namely MMP-2, PDGF, c-Myc, CCN1 and TGF-β1 (Fig. 4D). The high expression of MMP-2, PDGF, c-Myc and CCN1 indicates that the hair follicle stem cells are in the anagen phase for longer time [44–46], while the high expression of TGF-β1 indicates that the hair follicle stem cells enter the catagen, at which time the hair follicle begins to shrink and necrosis [47]. To further prove the regulation effect of ZCQ on DHT-injured HHDPs, we evaluated the separated and synergetic effects of Zn<sup>2+</sup>, Cu<sup>2+</sup> and Qu on the expression of the above five genes in HHDPs by real-time qPCR analysis. As shown in Fig. 4E, the injury induced by DHT was apparent as significant down-regulation of MMP-2, PDGF, c-Myc and CCN1, as well as up-regulation of TGF-β1 was shown in injured HHDPs. After the treatment with the combination of Zn<sup>2+</sup>, Cu<sup>2+</sup> and Qu, the expression of MMP-2, PDGF, c-Myc and CCN1 was significantly up-regulated, while the expression of TGF-β1 was significantly down-regulated. It is interesting to note that all Zn<sup>2+</sup> containing combinations including Zn<sup>2+</sup> alone also exhibited positive regulatory effect on the 5 genes expression, while Cu<sup>2+</sup> and Qu alone displayed a much weaker regulatory ability indicating Zn<sup>2+</sup> is the key factor for the protection of DHT-injured HHDPs and Cu<sup>2+</sup> and Qu only contribute to the synergetic effect by combining with Zn<sup>2+</sup> ions.

Finally, according to the analysis of the signaling pathways in the Kyoto Encyclopedia of Genes and Genomes database (KEGG) based on the results of RNA sequencing (Fig. 4F and Fig. S12), it was found that the combination of Zn<sup>2+</sup>, Cu<sup>2+</sup> and Qu (ZCQ) caused changes in more than 30 pathways, including the steroid biosynthesis pathway related to DHT [48–50], the TNF pathway related to inflammation [51], the TGF-β pathway related to hair follicle growth cycle [52], the VEGF and HIF-1 pathways related to angiogenesis [53,54], and the AMPK pathway

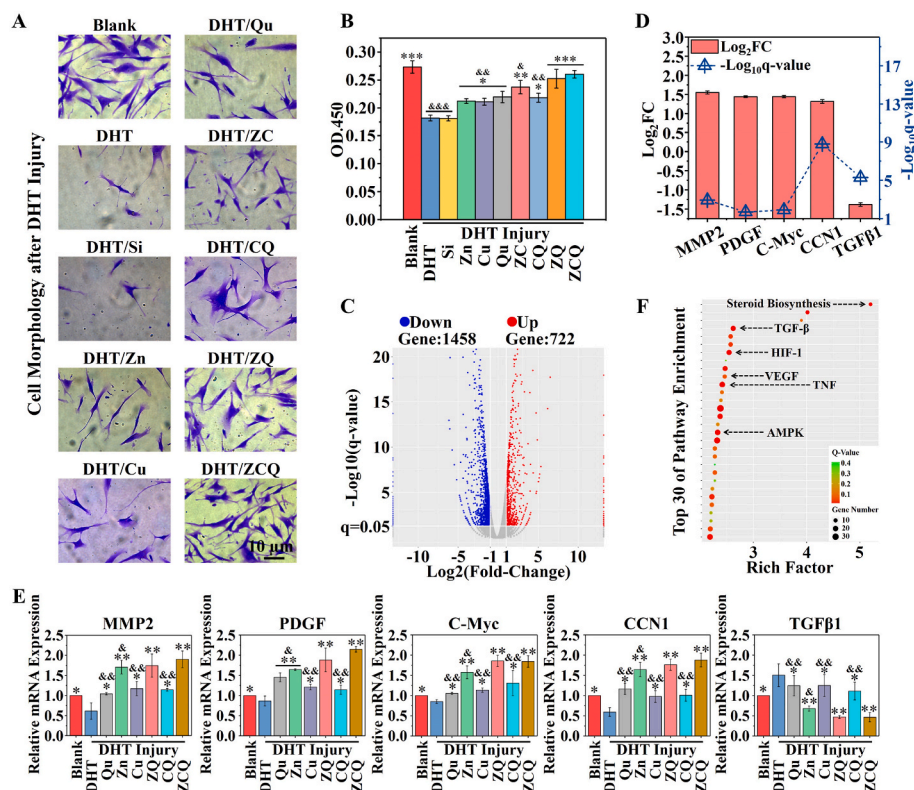


**Fig. 4.** Zn<sup>2+</sup>, Cu<sup>2+</sup> and Qu synergistically protect human hair follicle dermal papilla cells (HHDPs) from DHT attack. (A) Representative purple crystal staining images and (B) viability of DHT injured HHDPs with different treatments (Zn<sup>2+</sup>, Cu<sup>2+</sup>, SiO<sub>3</sub><sup>2-</sup>, Qu or their combinations (ZC, CQ, ZQ, ZCQ)) for 48 h (n = 6). (C) Sequencing analysis of DHT-injured HHDPs with or without ZCQ treatment for 72 h. Volcano plot shows 722 up-regulated and 1458 down-regulated genes in DHT-injured HHDPs after the treatment with ZCQ. (D) The expression of representative hair follicles related genes (MMP-2, PDGF, c-Myc, CCN1 and TGF-β1) from sequencing analysis. (E) qPCR analysis of the expression of hair follicle related markers in DHT injured HHDPs with different treatments (Zn<sup>2+</sup>, Cu<sup>2+</sup>, Qu or their combinations) for 72 h (n = 3). (F) KEGG pathway analysis of regulated genes in DHT-injured HHDPs after the treatment with ZCQ (\*p < 0.05, \*\*p < 0.01 and \*\*\*p < 0.001 vs. DHT. & < 0.05 and &&p < 0.01 vs. ZCQ.). (ZC: Zn<sup>2+</sup> and Cu<sup>2+</sup>; ZQ: Zn<sup>2+</sup> and Qu; CQ: Cu<sup>2+</sup> and Qu; ZCQ: Zn<sup>2+</sup> and Cu<sup>2+</sup> and Qu.) Blank: Normal HHDPs without DHT treatment.

related to skin regeneration [55]. Such results confirmed our hypothesis that ZCQ may have a systematic regulation effect and be able to treat AGA through multiple pathways with enhanced therapeutic effect.

### 3.5. The synergistic effect of $Zn^{2+}$ , $Cu^{2+}$ , and Qu on the regulation of macrophages *in vitro* and *in vivo*

The inflammatory cell model was constructed using Raw 264.7 macrophages treated with lipopolysaccharide (LPS), and the expression of pro-inflammatory cytokines (TNF- $\alpha$ , and IL-6) were evaluated by qPCR assay. As shown in Fig. 5A, all the combination including triple-components (ZCQ) and dual-components (ZC, ZQ, CQ) showed significant inhibitory effect on inflammation as the expression of TNF- $\alpha$  and IL-6 in ZCQ group was significantly lower than the single component treatment with  $Zn^{2+}$ ,  $Cu^{2+}$  or Qu alone, which suggests the unique synergistic effect of  $Zn^{2+}$ ,  $Cu^{2+}$  and Qu. Interestingly,  $Zn^{2+}$  and Qu alone also significantly reduced the expression of TNF- $\alpha$  and IL-6 in cells, and the combination of the  $Zn^{2+}$  and Qu (ZQ) generated a synergistic anti-inflammatory effect, which was ~10% higher than  $Zn^{2+}$  and Qu alone. More interestingly,  $Cu^{2+}$  alone significantly increased the expression of pro-inflammatory factors, which were slightly inhibited by the combination of  $Zn^{2+}$  (ZC) and completely inhibited by the combination of Qu (CQ) or  $Zn^{2+}$  and Qu (ZCQ).

Furthermore, the protective effects of  $Zn^{2+}$ ,  $Cu^{2+}$ , Qu and their combinations on the death of HHDPCs caused by LPS activated Raw 264.7 were evaluated in a co-culture system and analyzed using live/dead staining (Fig. 5C). A similar tendency was observed as either  $Zn^{2+}$  or Qu alone could slightly reverse the death of HHDPCs as compared to the Blank group, while  $Cu^{2+}$  alone showed an opposite effect. Unsurprisingly, the combination of each of them exhibited an enhanced protective effect as compared to the corresponding single component, and the protective effects produced by the dual-components combination were further enhanced by triple-components combination (ZCQ). Since the combination of  $Zn^{2+}$ ,  $Cu^{2+}$  and Qu (ZC, ZQ, CQ, and ZCQ) has better biological activity than the single components, we used the combination groups in the follow-up study.

Based on the above results, AGA mice were used to evaluate the synergistic effect of ZCQ/MN on inhibiting inflammation *in vivo* on day 3. Interestingly, ZCQ/MN significantly inhibited the early inflammatory response, and the number of macrophages in ZCQ/MN group was almost the same as that of healthy group. However, both Qu/MN and ZC/MN

could only slightly inhibit inflammation (Fig. S9). This result suggests that  $Zn^{2+}$ ,  $Cu^{2+}$ , and Qu indeed produce a synergistic effect to effectively inhibit the early inflammatory response of AGA.

### 3.6. The synergistic activation effect of $Zn^{2+}$ , $Cu^{2+}$ , and Qu on hair follicle cells and endothelial cells *in vitro* and *in vivo*

Apart from direct protection of the hair follicle stem cells from DHT attack or excessive inflammation, the activation of the undamaged peripheral hair follicle stem cells or endothelial cells to proliferate and migrate to the hair loss area is also important for hair re-growth in alopecia area. Thus, we further investigated the synergistic effect of  $Zn^{2+}$ ,  $Cu^{2+}$ , and Qu on the activity of HHDPCs and HUVECs. The cell viability of HHDPCs and HUVECs with the treatment of different groups was first investigated using CCK-8 assay. As shown in Fig. 6A, the combination of  $Zn^{2+}$ ,  $Cu^{2+}$  and Qu (ZC, ZQ, CQ, and ZCQ) significantly promoted the proliferation of HHDPCs on day 3 as compared to the Blank group, and no significant difference was shown among these groups at this time point. However, on day 5, the HHDPCs proliferation in the ZCQ group was significantly higher than that in any other groups. Similar to HHDPCs, significantly enhanced proliferation of HUVECs was observed in all treatment groups (ZC, ZQ, CQ and ZCQ) as compared with Blank group on day 5 (Fig. 6B). An interesting observation is that three  $Cu^{2+}$  containing groups (ZC, CQ, and ZCQ) showed higher stimulatory effect as compared to ZQ group, indicating the specific role of  $Cu^{2+}$  on the activation of HUVECs.

The migration performances of HHDPCs and HUVECs with the treatment of different groups were evaluated by *in vitro* scratch assay (Fig. 6C and D). A similar tendency was shown in both cells as all treatments (ZC, ZQ, CQ and ZCQ) promoted the migration of both HHDPCs and HUVECs, and ZCQ group revealed the best promotion activity. The quantitative statistical results (Fig. 6E and F) further confirmed the highest bioactivity of ZCQ in stimulating the migration of HHDPCs and HUVECs, while CQ was the second highest. When we compare the results of ZQ and CQ groups, we can see that CQ has higher activity in stimulate both cell migration than ZQ group.

Furthermore, we assessed the expression of hair follicle growth phase related genes (Hair follicles anagen phase: PDGF and C-Myc; Hair follicles telogen phase: TGF- $\beta$ 1.) in HHDPCs (Fig. S7). We found that only the combination containing  $Cu^{2+}$  and Qu including CQ and ZCQ could effectively increase the expression of PDGF and c-Myc, and decrease the

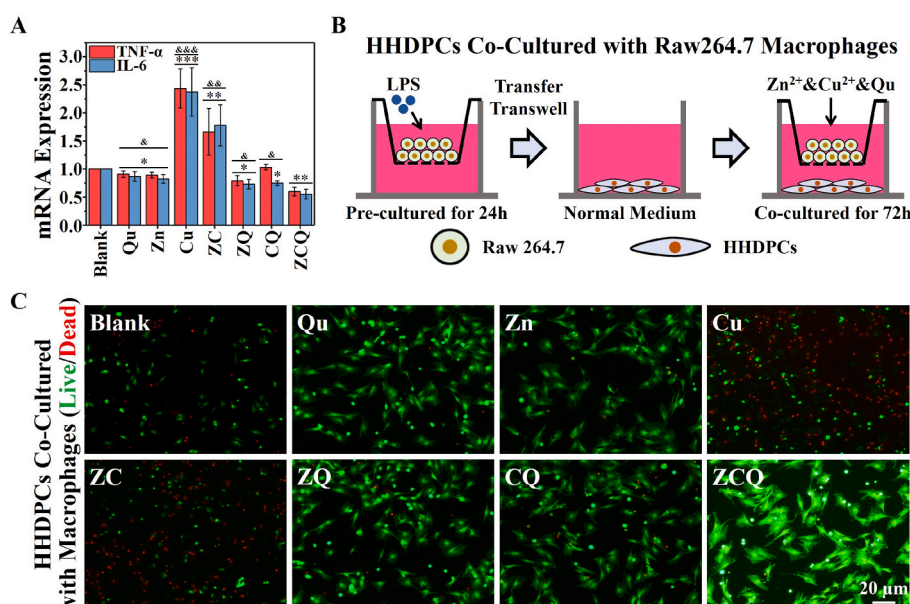


**Fig. 5.**  $Zn^{2+}$ ,  $Cu^{2+}$  and Qu synergistically alleviate inflammatory response of Raw 264.7 macrophage. (A) qPCR analysis of the expression of inflammation related markers (TNF- $\alpha$  and IL-6) in Raw 264.7 macrophage with different treatments for 72 h (n = 3). (B) Schematic representation of the co-culture of HHDPCs with Raw264.7 macrophages. (C) Representative live/dead staining images of HHDPCs after co-culture with pre-treated Raw 264.7 macrophages. Raw 264.7 were treated with different formulations after pre-stimulation with LPS for 24h (\*p < 0.05, \*\*p < 0.01 and \*\*\*p < 0.001 vs. Blank. &p < 0.05, &&p < 0.01 and &&&p < 0.001 vs. ZCQ.) Blank: Raw264.7 with LPS treatment.

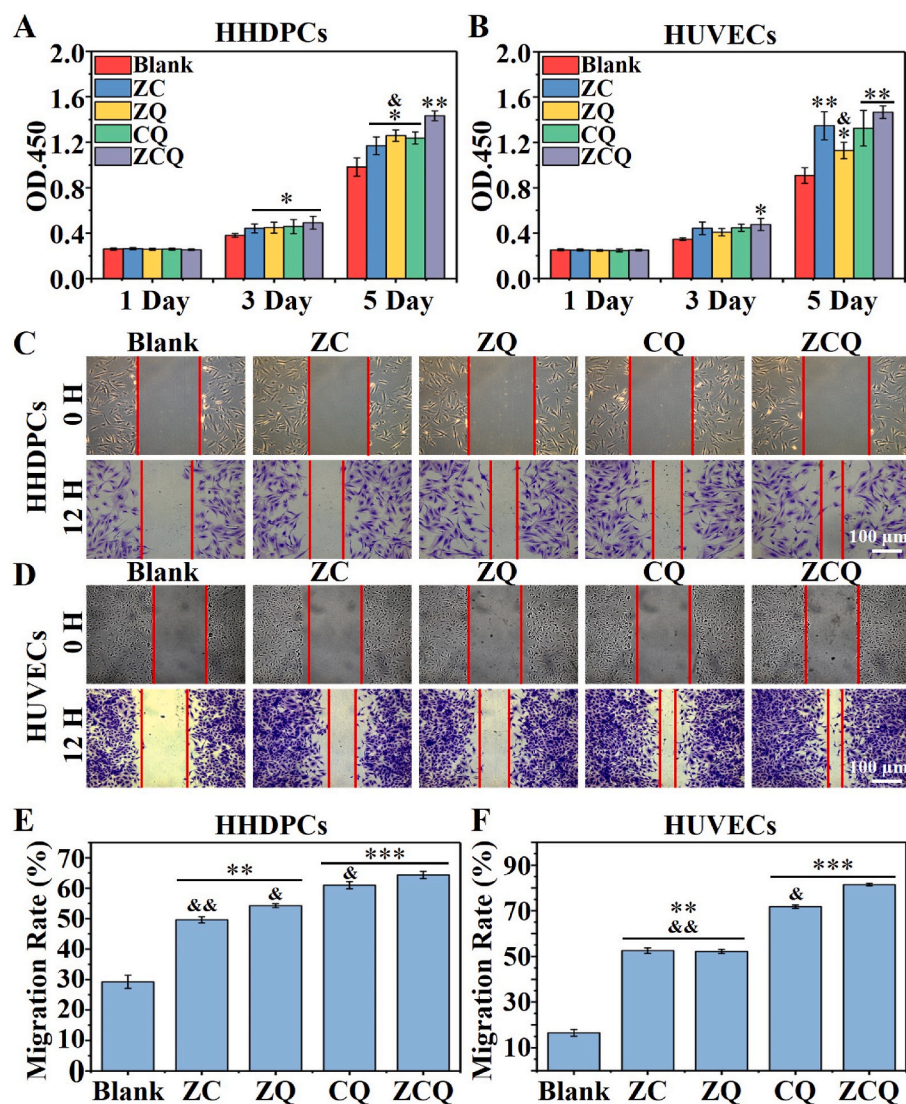


**Fig. 6.**  $Zn^{2+}$ ,  $Cu^{2+}$  and Qu synergistically promote the proliferation and migration activity of HHDPCs and HUVECs ( $n = 6$ ). (A, B) The proliferation of HHDPCs (A) and HUVECs (B) with different treatments (ZC, ZQ, CQ and ZCQ) for 1, 3, and 5 days. (C, D) The migration of HHDPCs (C) and HUVECs (D) with different treatments (ZC, ZQ, CQ and ZCQ) for 12 h. (E, F) Quantitative results of migration rate of HHDPCs (E) and HUVECs (F) (\* $p < 0.05$ , \*\* $p < 0.01$  and \*\*\* $p < 0.001$  vs. Blank. & $p < 0.05$  and && $p < 0.01$  vs. ZCQ.)

Blank: Normal HHDPCs and HUVECs cultured with MSCM and ECM medium, respectively.

expression of TGF- $\beta$ 1, and ZCQ group revealed higher regulation activity than CQ group. All these results suggest that the synergistic effect of  $Cu^{2+}$  and Qu plays a key role in the activation of hair follicle cells and endothelial cells around the hair loss area.

Therefore, we further investigated the activation effect of ZCQ/MN on endothelial and hair follicle cells in AGA mice at an early stage. Interestingly, on day 3, ZCQ/MN induced more hair follicle precursors and capillaries to regenerate in dermis than ZC/MN and Qu/MN groups (Figs. S10 and S11), indicating that the synergistic effect of  $Zn^{2+}$ ,  $Cu^{2+}$ , and Qu effectively activated damaged hair follicle cells and endothelial cells of AGA.

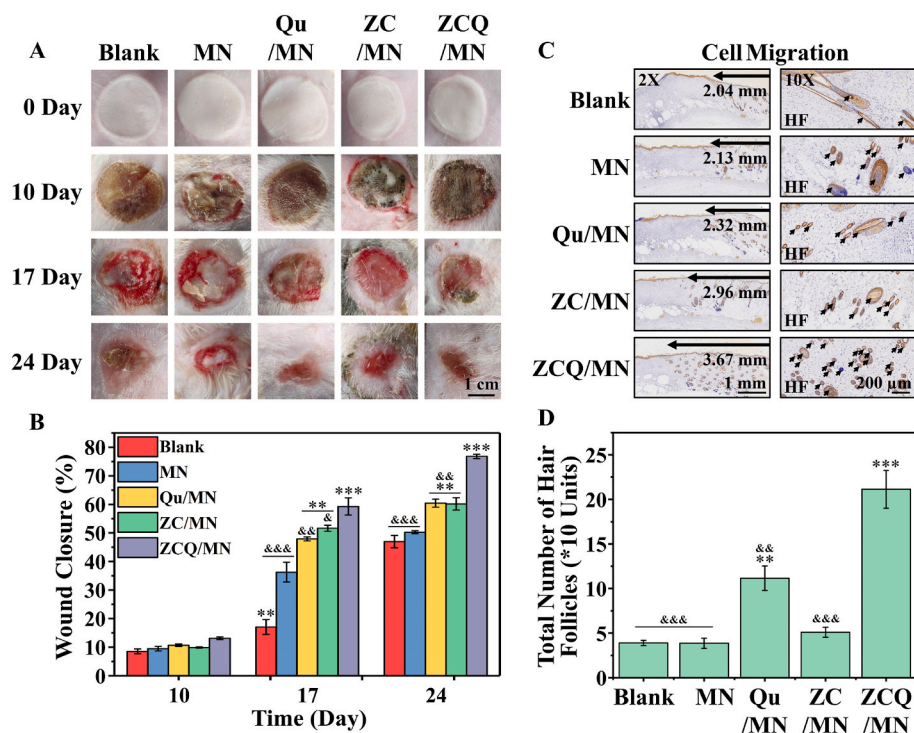
### 3.7. Effect of ZCQ/MN on hair follicle regeneration in rat burn model

Since the activation of undamaged hair follicles surrounding the hair loss area contributes to the hair regeneration in hair loss area, but it is difficult to separate the beneficial effect of ZCQ on the activation of undamaged hair follicles surrounding the hair loss area from the total therapeutic effects in the AGA mice model, we further used a deep third-degree rat burn model (all subcutaneous hair follicles in wound area were destroyed) to investigate the therapeutic effects of ZCQ/MN on the regeneration of hair follicles in burn areas, in which the hair follicle cells surrounding the burn area need to be activated and migrated to the wound area for hair regeneration. As shown in Fig. 7A, scalded wounds

in each group formed and gradually turned into large-area scabs from day 0 to day 10. The scabs then completely fell off and the wounds began to heal in all groups on day 17. On day 24, the wounds almost completely healed in ZCQ/MN group and a large amount of hair was observed surrounding the wound area. The quantitative analysis of wound closure revealed that Qu/MN, ZC/MN and ZCQ/MN groups exhibited a faster wound healing rate as compared with MN group on day 17 and 24. In particular, ZCQ/MN increased the wound healing rate by ~25% on day 17 and by ~26% on day 24 as compared to the Qu/MN and ZC/MN groups (Fig. 7B).

Histological analysis of H&E staining was further utilized and the images were taken to observe the progress of skin healing. As shown in Fig. S9, similar healing phases were observed in all groups on day 10 as the hair follicle tissue originally retained in the dermis disappeared, and the cells in the dermis layer were largely apoptotic, forming many holes in each group. However, on day 24, the dermal layer in ZC/MN group and ZCQ/MN group was almost completely healed with a new epidermal layer. In contrast, no visible epidermal layers were formed in Blank, MN and Qu/MN groups.

Furthermore, we used immunohistochemical staining of K19 to compare the hair growth rate at the fully healed wound site in each group on day 24. It is clearly shown that new hair follicle tissue began to appear at the edge of the wound and migrated from the outside to the inside. The migration rate of hair follicle stem cells was clearly higher in



ZCQ/MN, ZC/MN and Qu/MN groups as compared with Blank group, and the ZCQ/MN group showed the fastest migration rate, and more newly-formed hair follicles were observed in higher magnification images (Fig. 7C). The quantitative analysis confirmed the conclusion as the number of hair follicles at the wound edge in ZCQ/MN group was significantly higher than that in other groups (Fig. 7D). Interestingly, we found that ZC/MN mainly promoted the migratory ability of hair follicle cells, while Qu/MN mainly promoted the proliferative ability of hair follicle cells. These results indicate that different components in the ion-Qu combinations have different roles in regulating different cellular behaviors, and Zn–Cu ion combination mainly regulates the hair follicle cell migration, and the flavonoid Qu is critical for hair follicle cell proliferation, and the combination of the two creates the best effect for regulation of both migration and differentiation. An interesting phenomenon we observed in our *in vivo* results is that the migration distance in ZC/MN group was clearly longer as compared with that in Qu/MN group, while the fair follicles number in Qu/MN group was higher than that in ZC/MN group. This result suggests that although more hair follicle stem cells were activated migrating to the center of the wound area in ZC/MN groups, more hair follicles were grown out in the wound center in Qu/MN as compared to the ZC/MN group indicating a complex regulation mechanism of the hair regeneration (Fig. 7). To explain this phenomenon, the angiogenesis at the wound site on day 10 and 24 was assessed by CD31 immunohistochemical staining since blood vessels are critical for nutrients and closely related to the viability and growth of hair follicles [56]. As shown in Fig. S10, no newly-formed vessel was observed in all groups on day 10. However, on the 24th day, from the representative picture of CD31, it can be observed that a large number of new blood vessels appeared. The number of new blood vessels was significantly higher in ZCQ/MN, ZC/MN and Qu/MN, especially in ZCQ/MN group, as compared with Blank and MN groups. The quantitative analysis further confirmed that the number of new blood vessels in the ZCQ/MN group was the highest, and the Qu/MN group showed a higher number of blood vessels than that in the ZC/MN group indicating a higher activity of Qu in stimulating hair follicle growth than ion combinations by stimulating new blood vessel formation and the nutrient apply is a critical factor for hair regeneration (Fig. S11).

**Fig. 7.** ZCQ/MN promotes rapid healing and regeneration of hair follicles of rat burn wounds. (A) Representative optical images and (B) quantitation results of wound closure after treatment with different microneedles (MN, Qu/MN, ZC/MN, and ZCQ/MN) on the 0<sup>th</sup>, 10<sup>th</sup>, 17<sup>th</sup>, and 24<sup>th</sup> day. Blank was treated with medical gauze (n = 3). (C) Representative immunohistochemical staining images and (D) quantitation results of for cytokeratin 19 (K19) on the 24<sup>th</sup> day (n = 3) (\*\*p < 0.01, \*\*\*p < 0.001 vs. MN group. &p < 0.05, &&p < 0.01, &&&p < 0.001 vs. ZCQ/MN.) Blank: The burn rat treated with medical gauze.

#### 4. Discussion

The application of minoxidil as the main drug for clinical treatment of AGA is mainly based on its inhibitory effect on dihydrotestosterone (DHT), and does not directly affect other pathophysiological phenomena related to AGA, such as inflammation and growth viability of hair follicle stem cells. In addition, minoxidil is an organic compound that is insoluble in water, and it needs to be dissolved in an organic solvent such as propylene glycol for clinical applications. Due to the presence of these organic solvents, some patients may develop severe allergic dermatitis after use, resulting in aggravated hair loss [57]. So, one of the previous research focuses has been on adjusting the dose of the drug or developing new ways of delivering the drug to alleviate its side effects [58, 59]. Therefore, how to develop a method or drug that can not only efficiently promote hair regeneration, but also has good biocompatibility is important for AGA therapy. Based on this, we proposed the idea of a systemic intervention by simultaneous regulation of the main pathophysiological processes of AGA including excessive androgen attack, inflammation and loss of growth activity of hair follicle stem cells [60], and we believe that the simultaneous inhibition of DHT and inflammation, activation of hair follicle stem cells, and stimulation of angiogenesis to improve blood supply on hair follicle growth [56] together may be more effective to promote hair regeneration in AGA. To verify our hypothesis, we applied a combination therapy strategy using one organic drug quercetin and two bioactive metal ions such as Zn<sup>2+</sup>, Cu<sup>2+</sup>, and designed a new type of nanocomposite microneedles (ZCQ/MN) containing zinc-copper-quercetin-combined (Zn<sup>2+</sup>, Cu<sup>2+</sup> and Qu) nanospheres, in which the mesoporous nanospheres were functioning as the carrier of metal ions and Qu, and microneedles as the delivery tool for nanospheres. When the microneedle penetrates into the dermis of the skin, it dissolves rapidly and the remaining nanospheres in the dermis sustained release biologically active Zn<sup>2+</sup>, Cu<sup>2+</sup> and Qu. Our experiments confirmed that this combination therapy indeed significantly promoted hair regeneration in AGA mice. At present, microneedle patch has been widely used in the delivery of biological agents such as vaccines or insulin in clinical research [61]. Based on this, we believe that, after the determination of the optimal ratio of Zn<sup>2+</sup>, Cu<sup>2+</sup> and Qu

for human body, this composite microneedle patch may have potential for the clinical application in AGA treatment.

For the treatment of AGA, it is crucial to inhibit the conversion of testosterone to DHT *in vivo* and reduce the damage of DHT to hair follicle tissue [62,63]. Previous studies have found that  $Zn^{2+}$  and  $Cu^{2+}$  are essential elements for hair growth, and function as inhibitors of 5 $\alpha$ -reductase, which can reconvert DHT to testosterone [22,23]. However, the therapeutic effect of  $Zn^{2+}$  or  $Cu^{2+}$  alone on 5 $\alpha$ -reductase is not strong enough for the treatment of AGA. Therefore, we consider an ion combination approach by using the combination of  $Zn^{2+}$  and  $Cu^{2+}$  released from Zn/Cu dual-doped MSN to obtain a better DHT inhibition effect. In addition to the ion combination, based on previous finding that Qu could chelate with some metal ions (e.g.,  $Cu^{2+}$ ) and the chelation further enhanced the biological activity of metal ions [25,27,28], we proposed a combination approach consisting of ion-ion and ion-flavonoid synergetic actions. Our results indeed demonstrated that Qu enhanced the efficacy of  $Zn^{2+}$  or  $Cu^{2+}$  in inhibiting DHT (Fig. 4). The three components combination revealed the highest bioactivity in inhibiting the DHT damage to HHDPCs as compared to single component and dual-components groups. More interestingly, we found that  $Zn^{2+}$  alone significantly upregulated the expression of MMP-2, PDGF, c-Myc and CCN1 in DHT-injured HHDPCs indicating the promotion of a transition of the cells into anagen phase. Furthermore, the expression of TGF- $\beta$ 1 was downregulated indicating a delay of the cells into catagen phase. In contrast, Qu and  $Cu^{2+}$  alone only slightly regulated the expression of these genes (Fig. 4B). This result suggests that in the  $Zn^{2+}$ ,  $Cu^{2+}$  and Qu combination,  $Zn^{2+}$  plays a dominant role in suppressing DHT, while  $Cu^{2+}$  and Qu are more likely to be enhancers of  $Zn^{2+}$  ions. The DHT inhibition effect of  $Zn^{2+}$  might be ascribed to its regulating action on zinc-containing proteins such as zinc finger E-box binding homeobox 1 (ZEB1), which is directly related to DHT inhibitors and affects the content of DHT [64,65].

Apart from DHT attacking, persistent inflammation is also an inducement to AGA [66]. A large number of inflammatory cells (macrophages, T cells, etc.) gather around the hair follicle and penetrate into the dermal papilla and release inflammatory factors such as TNF- $\alpha$  and IL-6 [67]. These inflammatory factors attack the hair follicle stem cells and inactivate them completely. However, no evidence indicates the anti-inflammation ability of the existing drugs such as Minoxidil for the treatment of AGA. Previous studies have found that both  $Zn^{2+}$  and Qu have strong anti-inflammatory activity in many biological applications [17,25]. Therefore, we hypothesize that the combination of  $Zn^{2+}$  and Qu may synergistically suppress the inflammation in AGA. Our experiments confirmed that the combination of  $Zn^{2+}$  and Qu did significantly inhibit expression of inflammatory factors (TNF- $\alpha$  and IL-6) in macrophages as compared to  $Zn^{2+}$  and Qu alone. Interestingly, although we see that  $Cu^{2+}$  alone revealed a pro-inflammatory effect by stimulating expression of TNF- $\alpha$  and IL-6, the combination of  $Cu^{2+}$  with  $Zn^{2+}$  and Qu completely suppressed the original pro-inflammatory effect of  $Cu^{2+}$  and even displayed the best anti-inflammatory effect among all groups (Fig. 5). This result suggests a unique advantage of the combination approach of different ions and flavonoids, which may not only enhance the bioactivity, but also suppress the negative or toxic effects of individual components. The reason behind this might be the chelation between  $Cu^{2+}$  and Qu, which has been found to be able to convert the originally oxidative  $Cu^{2+}$  into  $Cu^{+}$  and reduced the possible effect of  $Cu^{2+}$ -induced oxidative stress [24,25,68]. Therefore, when  $Cu^{2+}$  was added to the combination of  $Zn^{2+}$  and Qu, the anti-inflammatory effect of  $Zn^{2+}$  and Qu was further enhanced by  $Cu^{2+}$ , while the pre-inflammatory effect of the  $Cu^{2+}$  was suppressed. This discovery broads the application prospects of both ions and flavonoids not only for enhancement of bioactivity, but also for suppression of side effects. Our findings indicate that the triple-components combination of  $Zn^{2+}$ ,  $Cu^{2+}$  and Qu not only showed stronger inhibition of DHT damage, but also more effective suppression of inflammation during AGA as compared to single-component or dual-components combination.

In addition to inhibiting the DHT attack and inflammation, enhancement of hair regeneration capacity is critical for AGA therapy, and activating the transition of hair follicle stem cells from telogen phase to anagen phase is one of the key factors for restarting hair regeneration [44]. Previous studies have shown that some exogenous growth factors such as IGF, PDGF, KGF, HGF, bFGF and C-Myc can stimulate the transition of hair follicle stem cells from telogen phase to anagen phase [69–73]. However, without the inhibition of DHT, growth factors alone can only relieve symptoms of mild AGA, but have little effect on treating AGA [74]. In our combination therapy,  $Zn^{2+}$  can not only suppress the generation of DHT in hair follicles, but also function as a specific activator of HHDPCs, which can effectively stimulate the transition of HHDPCs from the state of telogen to anagen and promote them to enter the growth phase by up-regulating the expression of some growth factors (IGF, PDGF, KGF, HGF, bFGF and C-Myc) [44,69,75]. However,  $Zn^{2+}$  single ions treatment is not strong enough to stimulate hair regeneration in AGA, and one of our hypotheses is that the combination of  $Zn^{2+}$  with  $Cu^{2+}$  and Qu together may synergistically enhance hair regeneration in AGA, since previous studies demonstrated that the combination of  $Cu^{2+}$  with amino acids could effectively activate the hair follicle stem cells in telogen phase and promote cell proliferation [76], and polyphenolic compounds (e.g., gallic acid and Qu) exhibit amino acid-like activity in some conditions [77,78], although it is unclear whether  $Cu^{2+}$ , Qu alone, or their combination with  $Zn^{2+}$  would have a regulatory effect on hair follicle stem cells in the telogen phase. The experimental results confirmed our speculation that the combination of  $Cu^{2+}$  and Qu stimulated the expression of PDGF and C-Myc which are markers of the anagen phase for hair follicle cells, and significantly down-regulated the expression of TGF- $\beta$ 1, which indicates an inhibitory effect on the transition of the normal hair follicle cells into the catagen phase. Although the  $Zn^{2+}$ - $Cu^{2+}$  combination (ZC) and the  $Zn^{2+}$ -Qu combination (ZQ) had no significant difference in regulating the expression of PDGF, C-Myc and TGF- $\beta$ 1 as compared with the Blank group, suggesting that  $Zn^{2+}$  alone may have no obvious regulatory effect on the expression of these three growth factors (Fig. S7), previous studies have shown that  $Zn^{2+}$  can stimulate hair follicle stem cells to enter the growth phase by up-regulating the expression of other growth factors such as IGF and HGF [44,69,75]. This explains the further activating effect of adding  $Zn^{2+}$  to the combination of Qu and  $Cu^{2+}$  in our study, which is mainly due to the synergistic effect based on the original effect of  $Zn^{2+}$  and the combination of Qu- $Cu^{2+}$ . This result indicates that the combination of  $Zn^{2+}$ ,  $Cu^{2+}$  and Qu not only has an effect on inhibiting androgen damage and inflammation, and the resulted apoptosis of hair follicle cells, but also has a synergistic effect on activating hair follicle cells. And this synergistic effect is achieved by activating hair follicle cells to upregulate (PDGF, and C-Myc) or downregulate (TGF- $\beta$ 1) the expression of related growth factors. After hair follicle cells in telogen phase are activated, the migration to the regenerating site is also a critical step in hair regeneration. We found that the combination of  $Zn^{2+}$ ,  $Cu^{2+}$  and Qu can not only activate the hair follicle cells in telogen phase to enter the anagen phase, but also enhance the proliferation and migration of the hair follicle cells (Fig. 7C and D). Interestingly, the  $Zn^{2+}$  and  $Cu^{2+}$  showed higher activity in promoting the migration of hair follicle cells, while Qu was more bioactive in promoting the proliferation of hair follicle cells. Since both  $Zn^{2+}$  and  $Cu^{2+}$  can promote the migration of HHDPCs, it is understandable that the combination of these two ions resulted in higher migration-stimulating activity than each single ions and Qu [26,44]. Furthermore, previous studies have shown that, unlike other skin-related cells such as fibroblasts and endothelial cells, the proliferation and migration ability of hair follicle cells is directly related to the cell growth cycle. The earlier the cells enter the anagen phase, the stronger their ability to proliferate and migrate [79]. This may be the main reason why the combination of  $Zn^{2+}$ ,  $Cu^{2+}$  and Qu can activate hair follicle cells to enter the anagen phase and promotes the migration of hair follicle cells simultaneously.

Besides the activation of hair follicle stem cells, adequate nutrients

supply is also essential for hair growth, which is mainly provided through the capillaries in hair follicles. A recent study has found that promoting vascularization at the site of hair loss may benefit hair regeneration [56]. However, this important issue is neglected in current developing strategies for treating AGA.  $\text{Cu}^{2+}$  is known to be bioactive in stimulating angiogenesis at a specific concentration range, and our previous study already revealed the synergistic effect of  $\text{Cu}^{2+}$  and Qu as a highly active chelate for promoting vascularization [26]. However, whether the addition of  $\text{Zn}^{2+}$  would affect the angiogenic ability of  $\text{Cu}^{2+}$ -Qu complex was a key issue to be clarified in this study, since the  $\text{Zn}^{2+}$  alone is not considered as an activator of angiogenesis [80]. Previous studies have shown that  $\text{Zn}^{2+}$  can enhance the angiogenic ability of other angiogenic materials, such as silicate and chitosan [44,81,82]. In our study, we also observed that, when  $\text{Zn}^{2+}$  was added to combination with  $\text{Cu}^{2+}$  and Qu (ZCQ), the viability and migration of HUVECs was further enhanced as compared with CQ. Therefore, we speculated that although  $\text{Zn}^{2+}$  alone is not active in stimulating angiogenesis, it could act as an enhancer to enhance the angiogenic ability of other angiogenesis activators such as  $\text{Cu}^{2+}$  and Qu. Interestingly, our results revealed that both  $\text{Zn}^{2+}$ - $\text{Cu}^{2+}$  and  $\text{Zn}^{2+}$ -Qu combinations stimulated the viability and migration of HUVECs, and the triple-components approach of  $\text{Zn}^{2+}$ ,  $\text{Cu}^{2+}$  and Qu combination showed the highest stimulation. The *in vivo* wound healing experiment also further confirmed the highest enhancement of new blood vessel formation by the  $\text{Zn}^{2+}$ ,  $\text{Cu}^{2+}$  and Qu triple combination, which suggests that indeed an effective stimulation of angiogenesis contributes to the significantly enhanced effectiveness of AGA treatment.

Considering the different roles of Qu and  $\text{Zn}^{2+}$ - $\text{Cu}^{2+}$  dual-ions released from to the ZCQ/MN nanocomposite in regulating the pathophysiological processes of AGA including androgens attack, inflammation, and lack of growth activity of hair follicle stem cells, the possible underlying mechanism is summarized in Fig. 8. First,  $\text{Zn}^{2+}$  protects hair follicle stem cells by inhibiting the production of steroid  $5\alpha$ -reductase through regulating the steroid biosynthesis pathway, thereby reducing the conversion of testosterone to DHT, in which Qu and  $\text{Cu}^{2+}$  act as enhancers of  $\text{Zn}^{2+}$  ions. Secondly, the combination of  $\text{Zn}^{2+}$  and Qu results in a synergistic inhibitory effect on the production of inflammatory factors (TNF- $\alpha$ , IL-6), and protects hair follicle stem cells from excessive inflammation, while  $\text{Cu}^{2+}$  acts as an enhancer of the Qu and  $\text{Zn}^{2+}$  ions. Thirdly, the combination of  $\text{Cu}^{2+}$  and Qu synergistically activates hair

follicle stem cells to re-enter anagen phase, so that the cells remain highly active and continue to proliferate, migrate and differentiate. Furthermore, the combination of  $\text{Cu}^{2+}$  and Qu synergistically activated endothelial cells and promotes angiogenesis in the skin to provide sufficient nutrients for the hair loss area and create a favorable growth environment for hair follicle regeneration, while  $\text{Zn}^{2+}$  acts as an enhancer of the  $\text{Cu}^{2+}$  and Qu in angiogenesis.

## 5. Conclusion

In this work, we proposed a combination therapy for AGA by the combination of a flavonoid (Qu) and two metal ions ( $\text{Zn}^{2+}$  and  $\text{Cu}^{2+}$ ), which are sustained delivered using a designed ZCQ/MN nanocomposite microneedle patch. The results revealed that this combination therapy is effective in treating AGA in a mouse model, and the synergistic action of Qu,  $\text{Zn}^{2+}$  and  $\text{Cu}^{2+}$  is the key for the enhancement of hair growth in AGA mouse, in which different single components and two components' combinations play different roles simultaneously in targeting different pathophysiological processes of the AGA including inhibiting excess androgen, inhibiting inflammation and promoting hair follicle regeneration. This study demonstrated that the systematic intervention based on multi-components nanocomposite biomaterials simultaneously targeting three pathophysiological processes is an effective way to treat AGA, which may be applied for the development of novel therapy for clinical treatment of AGA and other type of hair loss.

## Ethics approval and consent to participate

All animal operations were performed in accordance with the guidelines for the care and use of laboratory animals in Shanghai Jiao Tong University (Shanghai, China), and approved by the Animal Ethics Committee of the Sixth People's Hospital Affiliated to Shanghai Jiao Tong University School of Medicine (Shanghai, China).

## CRediT authorship contribution statement

**Zhaowenbin Zhang:** Formal analysis, Data curation, Writing – original draft, drew up the plan, carried out the experiments, analyzed the experimental data, and wrote the manuscript. **Wenbo Li:** Formal analysis, Data curation, Writing – original draft, drew up the plan,

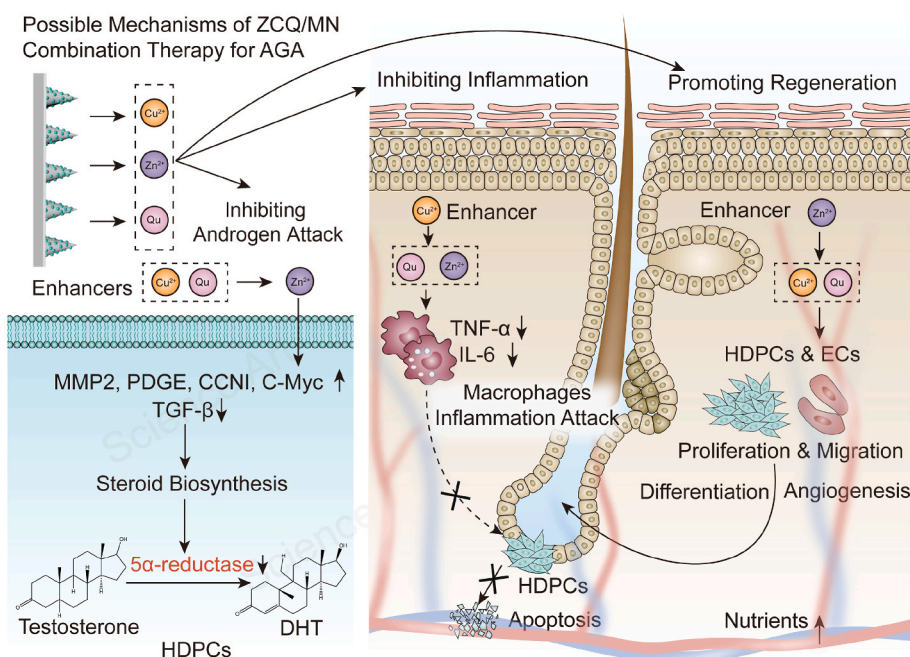


**Fig. 8.** The possible mechanism of ZCQ/MN combination therapy for AGA: (a)  $\text{Zn}^{2+}$  inhibits DHT damage to hair follicle stem cells (HDPCs) and Qu and  $\text{Cu}^{2+}$  act as enhancers of the  $\text{Zn}^{2+}$  ions. (b) The combination of  $\text{Zn}^{2+}$  and Qu synergistically inhibits the inflammation and prevents the inflammation-induced death of hair follicle stem cells, while  $\text{Cu}^{2+}$  acts as an enhancer of the  $\text{Zn}^{2+}$  and Qu action. (c) The combination of  $\text{Cu}^{2+}$  and Qu on one hand enhances the proliferation and migration of hair follicle stem cells, and on the other hand activates endothelial cells (ECs) and stimulates angiogenesis for improved nutrients supply, thereby promoting the hair growth, while  $\text{Zn}^{2+}$  acts as an enhancer of the action of the  $\text{Cu}^{2+}$  and Qu.

carried out the experiments, analyzed the experimental data, and wrote the manuscript. **Di Chang:** Formal analysis, Data curation, performed the animal experiments and participated in data analysis. **Ziqin Wei:** Formal analysis, Data curation, performed the animal experiments and participated in data analysis. **Endian Wang:** Formal analysis, Data curation, performed the animal experiments and participated in data analysis. **Jing Yu:** Formal analysis, Data curation, performed the animal experiments and participated in data analysis. **Yuze Xu:** Formal analysis, Data curation, performed the animal experiments and participated in data analysis. **Yumei Que:** Formal analysis, Data curation, performed the animal experiments and participated in data analysis. **Yanxin Chen:** Formal analysis, Data curation, performed the animal experiments and participated in data analysis. **Chen Fan:** Formal analysis, Data curation, performed the animal experiments and participated in data analysis. **Bing Ma:** Formal analysis, Data curation, performed the animal experiments and participated in data analysis. **Yanling Zhou:** Formal analysis, Data curation, performed the animal experiments and participated in data analysis. **Zhiguang Huan:** Formal analysis, Data curation, performed the animal experiments and participated in data analysis. **Chen Yang:** Data curation, Supervision, discussed the data. and initiated, designed, and supervised the study and revised the manuscript. **Feng Guo:** Data curation, Supervision, discussed the data. and initiated, designed, and supervised the study and revised the manuscript. **Jiang Chang:** Data curation, Supervision, discussed the data. and initiated, designed, and supervised the study and revised the manuscript.

#### Declaration of competing interest

The authors declare that they have no known competing financial interests or personal relationships that could have appeared to influence the work reported in this paper.

#### Acknowledgements

This research was supported by Science and Technology Commission of Shanghai Municipality (No. 20S31904500), the National Natural Science Foundation of China (No. 81772078 and No. 82172200 and No.31900945 and No.82100427), Shanghai 2022 "Science and Technology Innovation Action Plan" biomedical science and technology support special project (No. 22S31902800), Shanghai Science and Technology Commission INTERNATIONAL COOPERATION Project (No. 21520712300), the seed grants from the Wenzhou Institute, University of Chinese Academy of Sciences (WIUCASQD2020013, WIUCASQD2021030), and the founding from the First Affiliated Hospital of Wenzhou Medical University.

#### Appendix A. Supplementary data

Supplementary data to this article can be found online at <https://doi.org/10.1016/j.bioactmat.2022.12.007>.

#### References

- M. Znidaric, Z.M. Zurga, U. Maver, Design of in vitro hair follicles for different applications in the treatment of alopecia-A review, *Biomedicines* 9 (4) (2021) 19.
- F. Lolli, F. Pallotti, A. Rossi, M.C. Fortuna, G. Caro, A. Lenzi, A. Sansone, F. Lombardo, Androgenetic alopecia: a review, *Endocrine* 57 (1) (2017) 9–17.
- A. Rossi, A. D'Arino, F. Pigliacelli, G. Caro, M. Muscianese, M.C. Fortuna, M. Carlesimo, The diagnosis of androgenetic alopecia in children: considerations of pathophysiological plausibility, *Australas. J. Dermatol.* 60 (4) (2019) E279–E283.
- O.T. Norwood, Incidence of female androgenetic alopecia (female pattern alopecia), *Dermatol. Surg.* 27 (1) (2001) 53–54.
- W.S. Lee, H.J. Lee, Characteristics of androgenetic alopecia in asian, *Ann. Dermatol.* 24 (3) (2012) 243–252.
- F.M. Sakr, A.M. Gado, H.R. Mohammed, A.N.I. Adam, Preparation and evaluation of a multimodal minoxidil microemulsion versus minoxidil alone in the treatment of androgenic alopecia of mixed etiology: a pilot study, *Drug Des. Dev. Ther.* 7 (2013) 413–423.
- T. Kiguradze, W.H. Temps, R. Kantor, S. Lyon, D.P. West, S.M. Belknap, Evaluation of risk of SSRI-associated impotence and low libido in men exposed to finasteride, *J. Am. Acad. Dermatol.* 74 (5) (2016). AB221-AB221.
- N. Kash, M. Leavitt, A. Leavitt, S.D. Hawkins, R.B. Roopani, Clinical patterns of hair loss in men is dihydrotestosterone the only culprit? *Dermatol. Clin.* 39 (3) (2021) 361–370.
- J.A. Carlson, J. Malysz, J. Schwartz, Female-patterned alopecia in teenage brothers with unusual histologic features, *J. Cutan. Pathol.* 33 (11) (2006) 741–748.
- C.M. Magro, A. Rossi, J. Poe, S. Manhas-Bhutani, N. Sadick, The role of inflammation and immunity in the pathogenesis of androgenetic alopecia, *J. Drugs Dermatol.* JDD 10 (12) (2011) 1404–1411.
- A. Ogunbiyi, B. Adedokun, Perceived aetiological factors of folliculitis keloidalis nuchae (acne keloidalis) and treatment options among Nigerian men, *Br. J. Dermatol.* 173 (2015) 22–25.
- Y.C. Yang, H.C. Fu, C.Y. Wu, K.T. Wei, K.E. Huang, H.Y. Kang, Androgen receptor accelerates premature senescence of human dermal papilla cells in association with DNA damage, *PLoS One* 8 (11) (2013).
- J. Griggs, R.M. Trueb, M. Dias, M. Hordinsky, A. Tosti, Fibrosing alopecia in a pattern distribution, *J. Am. Acad. Dermatol.* 85 (6) (2021) 1557–1564.
- H.M. Almohanna, A.A. Ahmed, J.P. Tsalalis, A. Tosti, The role of vitamins and minerals in hair loss: a review, *Dermatol. Ther.* 9 (1) (2019) 51–70.
- A.M. Finner, Nutrition and hair deficiencies and supplements, *Dermatol. Clin.* 31 (1) (2013) 167–+.
- Y. Zhang, M.L. Chang, F. Bao, M. Xing, E. Wang, Q. Xu, Z.G. Huan, F. Guo, J. Chang, Multifunctional Zn doped hollow mesoporous silica/polycaprolactone electrospun membranes with enhanced hair follicle regeneration and antibacterial activity for wound healing, *Nanoscale* 11 (13) (2019) 6315–6333.
- G.Y. Guo, Q. Xu, C.Z. Zhu, J.L. Yu, Q.J. Wang, J. Tang, Z.G. Huan, H. Shen, J. Chang, X.L. Zhang, Dual-temporal bidirectional immunomodulation of Cu-Zn Bilayer nanofibrous membranes for sequentially enhancing antibacterial activity and osteogenesis, *Appl. Mater. Today* 22 (2021).
- L. Pickart, The human tri-peptide GHK and tissue remodeling, *J. Biomater. Sci. Polym. Ed.* 19 (8) (2008) 969–988.
- J. Makowska, A. Tesmar, D. Wyrzykowski, L. Chmurzynski, Investigation of the binding properties of the cosmetic peptide argireline and its derivatives towards copper(II) ions, *J. Solut. Chem.* 47 (1) (2018) 80–91.
- L. Pickart, A. Margolina, Regenerative and protective actions of the GHK-Cu peptide in the light of the new gene data, *Int. J. Mol. Sci.* 19 (7) (2018).
- C.T. Wu, Y.H. Zhou, M.C. Xu, P.P. Han, L. Chen, J. Chang, Y. Xiao, Copper-containing mesoporous bioactive glass scaffolds with multifunctional properties of angiogenesis capacity, osteostimulation and antibacterial activity, *Biomaterials* 34 (2) (2013) 422–433.
- M.S. Fahim, M. Wang, M.F. Sutcu, Z. Fahim, Zinc arginine, a 5-Alpha-reductase inhibitor, reduces rat ventral prostate weight and DNA without affecting testicular function, *Andrologia* 25 (6) (1993) 369–375.
- Y. Sugimoto, I. Lopezsolache, F. Labrie, V. Luethe, Cations inhibit specifically type-I 5-Alpha-reductase found in human SKIN, *J. Invest. Dermatol.* 104 (5) (1995) 775–778.
- S. Selvaraj, S. Krishnaswamy, V. Devashya, S. Sethuraman, U.M. Krishnan, Flavonoid-metal ion complexes: a novel class of therapeutic agents, *Med. Res. Rev.* 34 (4) (2014) 677–702.
- M.M. Kasprzak, A. Erxleben, J. Ochocki, Properties and applications of flavonoid metal complexes, *RSC Adv.* 5 (57) (2015) 45853–45877.
- Z.W.B. Zhang, Q.X. Dai, Y. Zhang, H. Zhuang, E.D. Wang, Q. Xu, L.L. Ma, C.T. Wu, Z.G. Huan, F. Guo, J. Chang, Design of a multifunctional biomaterial inspired by ancient Chinese medicine for hair regeneration in burned skin, *ACS Appl. Mater. Interfaces* 12 (11) (2020) 12489–12499.
- Z. Zhang, Y. Zhang, W. Li, L. Ma, E. Wang, M. Xing, Y. Zhou, Z. Huan, F. Guo, J. Chang, Curcumin/Fe-SiO<sub>2</sub> nano composites with multi-synergistic effects for scar inhibition and hair follicle regeneration during burn wound healing, *Appl. Mater. Today* 23 (2021), 101065.
- Y. Liu, M. Guo, Studies on transition metal-quercetin complexes using electrospay ionization tandem mass spectrometry, *Molecules* 20 (5) (2015) 8583–8594.
- B. Iqbal, J. Ali, S. Baboota, Recent advances and development in epidermal and dermal drug deposition enhancement technology, *Int. J. Dermatol.* 57 (6) (2018) 646–660.
- P. Mishra, M. Handa, R.R. Ujjwal, V. Singh, P. Kesharwani, R. Shukla, Potential of nanoparticulate based delivery systems for effective management of alopecia, *Colloids Surf. B Biointerfaces* 208 (2021).
- L.A.F. Afione, C.Y. Ushirobira, D.P.P. Barbosa, P.E.N. de Souza, M.I.G. Leles, M. Cunha, G.M. Gelfuso, M.A.G. Soler, T. Gratieri, Novel iron oxide nanocarriers loading finasteride or dutasteride: enhanced skin penetration for topical treatment of alopecia, *Int. J. Pharm.* 587 (2020).
- O.A.A. Ahmed, W.Y. Rizq, Finasteride nano-transferosomal gel formula for management of androgenetic alopecia: ex vivo investigational approach, *Drug Des. Dev. Ther.* 12 (2018) 2259–2265.
- Y. Zhang, C. Huang, J. Chang, Ca-Doped mesoporous SiO<sub>2</sub>/dental resin composites with enhanced mechanical properties, bioactivity and antibacterial properties, *J. Mat. Chem. B* 6 (3) (2018) 477–486.
- X. Cai, Z. Fang, J. Dou, A. Yu, G. Zhai, Bioavailability of quercetin: problems and promises, *Curr. Med. Chem.* 20 (20) (2013) 2572–2582.
- S. Sapino, E. Ugazio, L. Gastaldi, I. Miletto, G. Berlier, D. Zonari, S. Oliaro-Bosso, Mesoporous silica as topical nanocarriers for quercetin: characterization and in vitro studies, *Eur. J. Pharm. Biopharm.* 89 (2015) 116–125.
- L. Das, M. Kaurav, R.S. Pandey, Phospholipid-polymer hybrid nanoparticle-mediated transfollicular delivery of quercetin: prospective implement for the

- treatment of androgenic alopecia, *Drug Dev. Ind. Pharm.* 45 (10) (2019) 1654–1663.
- [37] J. Monkare, M.R. Nejadnik, K. Baccouche, S. Romeijn, W. Jiskoot, J.A. Bouwstra, IgG-loaded hyaluronan-based dissolving microneedles for intradermal protein delivery, *J. Contr. Release* 218 (2015) 53–62.
- [38] W.J. Yu, G.H. Jiang, Y. Zhang, D.P. Liu, B. Xu, J.Y. Zhou, Polymer microneedles fabricated from alginate and hyaluronate for transdermal delivery of insulin, *Mater. Sci. Eng. C Mater. Biol. Appl.* 80 (2017) 187–196.
- [39] N.A.M. Kamal, T.M.T. Mahmood, I. Ahmad, S. Ramli, Improving rate of gelatin/carboxymethylcellulose dissolving microneedle for transdermal drug delivery, *Sains Malays.* 49 (9) (2020) 2269–2279.
- [40] S.S. Cao, Y.X. Wang, M. Wang, X.Y. Yang, Y.J. Tang, M.L. Pang, W.X. Wang, L. Chen, C.B. Wu, Y.H. Xu, Microneedles mediated bioinspired lipid nanocarriers for targeted treatment of alopecia, *J. Contr. Release* 329 (2021) 1–15.
- [41] M. Jin, Y.L. Chen, X.F. He, Y.P. Hou, Z.H. Chan, R.Y. Zeng, Amelioration of androgenetic alopecia by algal oligosaccharides prepared by deep-sea bacterium biodegradation, *Front. Microbiol.* 11 (2020).
- [42] D. Kim, B. Landmead, S.L. Salzberg, HISAT: a fast spliced aligner with low memory requirements, *Nat. Methods* 12 (4) (2015), 357–U121.
- [43] T. Chen, Z. Zhang, D. Weng, L. Lu, X. Wang, M. Xing, H. Qiu, M. Zhao, L. Shen, Y. Zhou, J. Chang, H.-P. Li, Ion therapy of pulmonary fibrosis by inhalation of ionic solution derived from silicate bioceramics, *Bioact. Mater.* 6 (10) (2021) 3194–3206.
- [44] Z. Zhang, W. Li, Y. Liu, Z. Yang, L. Ma, H. Zhuang, E. Wang, C. Wu, Z. Huan, F. Guo, J. Chang, Design of a biofluid-absorbing bioactive sandwich-structured Zn–Si bioceramic composite wound dressing for hair follicle regeneration and skin burn wound healing, *Bioact. Mater.* 6 (7) (2021) 1910–1920.
- [45] Y.K. Sung, M.H. Kwack, S.R. Kim, M.K. Kim, J.C. Kim, Transcriptional activation of CCN1 and CCN2, targets of canonical Wnt signal, by ascorbic acid 2-phosphate in human dermal papilla cells, *J. Dermatol. Sci.* 49 (3) (2008) 256–259.
- [46] A.M. Mahmoud, M.M. Ali, High glucose and advanced glycation end products induce CD147-mediated MMP activity in human adipocytes, *Cells* 10 (8) (2021) 16.
- [47] Y.S. Xie, K.J. McElwee, G.R. Owen, L. Hakkinen, H.S. Larjava, Integrin beta 6-deficient mice show enhanced keratinocyte proliferation and retarded hair follicle regression after depilation, *J. Invest. Dermatol.* 132 (3) (2012) 547–555.
- [48] D.S. Yamashita, D.A. Holt, H.J. Oh, D. Shah, H.K. Yen, M. Brandt, M.A. Levy, 3-carboxy-20-keto steroids are dual uncompetitive inhibitors of human steroid 5 alpha-reductase types 1 and 2, *Bioorg. Med. Chem.* 4 (9) (1996) 1481–1485.
- [49] M. Jarman, H.J. Smith, P.J. Nicholls, C. Simons, Inhibitors of enzymes of androgen biosynthesis: cytochrome P450(17 alpha) and 5 alpha-steroid reductase, *Nat. Prod. Rep.* 15 (5) (1998) 495–512.
- [50] V.S. Langlois, D.P. Zhang, G.M. Cooke, V.L. Trudeau, Evolution of steroid-5 alpha-reductases and comparison of their function with 5 beta-reductase, *Gen. Comp. Endocrinol.* 166 (3) (2010) 489–497.
- [51] A.Y. Kim, J.H. Ha, S.N. Park, Selective release system for antioxidative and anti-inflammatory activities using H2O2-responsive therapeutic nanoparticles, *Biomacromolecules* 18 (10) (2017) 3197–3206.
- [52] Z.Y. Wu, L.Z. Sun, G.Y. Liu, H.L. Liu, H.Z. Liu, Z.J. Yu, S. Xu, F.C. Li, Y.H. Qin, Hair follicle development and related gene and protein expression of skins in Rex rabbits during the first 8 weeks of life, *Asian-Australas. J. Anim. Sci.* 32 (4) (2019) 477–484.
- [53] A. Herman, A.P. Herman, Mechanism of action of herbs and their active constituents used in hair loss treatment, *Fitoterapia* 114 (2016) 18–25.
- [54] Y.H. Zhou, S.W. Han, L. Xiao, P.P. Han, S.F. Wang, J. He, J. Chang, C.T. Wu, Y. Xiao, Accelerated host angiogenesis and immune responses by ion release from mesoporous bioactive glass, *J. Mat. Chem. B* 6 (20) (2018) 3274–3284.
- [55] P. Zhao, B.-D. Sui, N. Liu, Y.-J. Lv, C.-X. Zheng, Y.-B. Lu, W.-T. Huang, C.-H. Zhou, J. Chen, D.-L. Pang, D.-D. Fei, K. Xuan, C.-H. Hu, Y. Jin, Anti-aging pharmacology in cutaneous wound healing: effects of metformin, resveratrol, and rapamycin by local application, *Aging Cell* 16 (5) (2017) 1083–1093.
- [56] A. Yuan, F. Xia, Q. Bian, H. Wu, Y. Gu, T. Wang, R. Wang, L. Huang, Q. Huang, Y. Rao, D. Ling, F. Li, J. Gao, Ceria nanzyme-integrated microneedles reshape the perifollicular microenvironment for androgenetic alopecia treatment, *ACS Nano* 15 (8) (2021) 13759–13769.
- [57] E.S. Friedman, P.M. Friedman, D.E. Cohen, K. Washenik, Allergic contact dermatitis to topical minoxidil solution: etiology and treatment, *J. Am. Acad. Dermatol.* 46 (2) (2002) 309–312.
- [58] S.S. Ocampo-Garza, G. Fabbrocini, J. Ocampo-Candiani, E. Cinelli, A. Villani, Micro needling: a novel therapeutic approach for androgenetic alopecia, *A Review of Literature, Dermatol. Ther.* 33 (6) (2020).
- [59] A.K. Jha, M. Zeeshan, A. Singh, P.K. Roy, Platelet-rich plasma with low dose oral minoxidil (1.25mg versus 2.5mg) along with trichoscopic pre- and post-treatment evaluation, *J. Cosmet. Dermatol.* 20 (10) (2021) 3220–3226.
- [60] W. Cranwell, R. Sinclair, Male androgenetic alopecia, in: K.R. Feingold, B. Anawalt, A. Boyce, G. Chrousos, W.W. de Herder, K. Dhatriya, K. Dungan, J.M. Hershman, J. Hofland, S. Kalra, G. Kaltsas, C. Koch, P. Kopp, M. Korbonits, C.S. Kovacs, W. Kuohung, B. Laferrère, M. Levy, E.A. McGee, R. McLachlan, J.E. Morley, M. New, J. Purnell, R. Sahay, F. Singer, M.A. Sperling, C.A. Stratakis, D.L. Trencle, D.P. Wilson (Eds.), *Endotext*, MDText.Com, Inc. Copyright © 2000–2021, MDText.com, Inc., South Dartmouth (MA), 2000.
- [61] K.J. Lee, S.S. Jeong, D.H. Roh, D.Y. Kim, H.-K. Choi, E.H. Lee, A practical guide to the development of microneedle systems - in clinical trials or on the market, *Int. J. Pharm.* 573 (2020).
- [62] J.I. Kang, S.C. Kim, S.C. Han, H.J. Hong, Y.J. Jeon, B. Kim, Y.S. Koh, E.S. Yoo, H. K. Kang, Hair-loss preventing effect of grateloupia elliptica, *Biomol. Ther.* 20 (1) (2012) 118–124.
- [63] D.L. Fu, J.F. Huang, K.T. Li, Y.X. Chen, Y. He, Y. Sun, Y.L. Guo, L.J. Du, Q. Qu, Y. Miao, Z.Q. Hu, Dihydrotestosterone-induced hair regrowth inhibition by activating androgen receptor in C57BL6 mice simulates androgenetic alopecia, *Biomed. Pharmacother.* 137 (2021).
- [64] D. Herrera, O. Orellana-Serradell, P. Villar, M.J. Torres, R. Paciucci, E.A. Castellon, H.R. Contreras, Silencing of the transcriptional factor ZEB1 alters the steroidogenic pathway, and increases the concentration of testosterone and DHT in DU145 cells, *Oncol. Rep.* 41 (2) (2019) 1275–1283.
- [65] Y.F. Tang, M.Q. Fan, Y.J. Choi, Y.H. Yu, G. Yao, Y.Y. Deng, S.H. Moon, E.K. Kim, Sika deer (*Cervus nippon*) velvet antler extract attenuates prostate cancer in xenograft model, *Biosci. Biotech. Biochem.* 83 (2) (2019) 348–356.
- [66] Y.F. Mahe, J.F. Michelet, N. Billoni, F. Jarrousse, B. Buan, S. Commo, D. Saint-Leger, B.A. Bernard, Androgenetic alopecia and microinflammation, *Int. J. Dermatol.* 39 (8) (2000) 576–584.
- [67] C. Jaworsky, A.M. Kligman, G.F. Murphy, Characterization of inflammatory infiltrates in male pattern alopecia - implications for pathogenesis, *Br. J. Dermatol.* 127 (3) (1992) 239–246.
- [68] L.T. Rael, N.K.R. Rao, G.W. Thomas, R. Bar-Or, C.G. Curtis, D. Bar-Or, Combined cupric- and cuprous-binding peptides are effective in preventing IL-8 release from endothelial cells and redox reactions, *Biochem. Biophys. Res. Commun.* 357 (2) (2007) 543–548.
- [69] J. Li, Z.H. Yang, Z. Li, L. Gu, Y. Wang, C. Sung, Exogenous IGF-1 promotes hair growth by stimulating cell proliferation and down regulating TGF-beta 1 in C57BL/6 mice in vivo, *Growth Hormone IGF Res.* 24 (2–3) (2014) 89–94.
- [70] Y. Tomita, M. Akiyama, H. Shimizu, PDGF isoforms induce and maintain anagen phase of murine hair follicles, *J. Dermatol. Sci.* 43 (2) (2006) 105–115.
- [71] T. Jindo, R. Tsuboi, K. Takamori, H. Ogawa, Local injection of hepatocyte growth factor scatter factor (HGF/SF) alters cyclic growth of murine hair follicles, *J. Invest. Dermatol.* 110 (4) (1998) 338–342.
- [72] N. Wang, T. Yang, J. Li, M.X. Lei, J.Z. Shi, W.M. Qiu, X.H. Lian, The expression and role of c-Myc in mouse hair follicle morphogenesis and cycling, *Acta Histochem.* 114 (3) (2012) 199–206.
- [73] S.O. Park, B.S. Park, G.Y. Noh, Action mechanism of natural plant extracts for hair loss prevention and hair growth promotion in C57BL/6 mice, *Int. J. Pharmacol.* 11 (6) (2015) 588–595.
- [74] A.P. Sclafani, Platelet-Rich fibrin matrix (PRFM) for androgenetic alopecia, *Facial Plast. Surg.* 30 (2) (2014) 219–224.
- [75] A.G. Hall, S.L. Kelleher, B. Lonnerdal, A.F. Philipps, A graded model of dietary zinc deficiency: effects on growth, insulin-like growth factor-1, and the glucose/insulin axis in weanling rats, *J. Pediatr. Gastroenterol. Nutr.* 41 (1) (2005) 72–80.
- [76] H.K. Pyo, H.G. Yoo, C.H. Won, S.H. Lee, Y.J. Kang, H.C. Eun, K.H. Cho, K.H. Kim, The effect of tripeptide-copper complex on human hair growth in vitro, *Arch Pharm. Res. (Seoul)* 30 (7) (2007) 834–839.
- [77] M. Akagawa, K. Suyama, Amine oxidase-like activity of polyphenols - mechanism and properties, *Eur. J. Biochem.* 268 (7) (2001) 1953–1963.
- [78] Y. Asano, K. Yasukawa, Identification and development of amino acid oxidases, *Curr. Opin. Chem. Biol.* 49 (2019) 76–83.
- [79] B. Zhu, T. Xu, Z.P. Zhang, N. Ta, X.Y. Gao, L.H. Hui, X.D. Guo, D.J. Liu, Transcriptome sequencing reveals differences between anagen and telogen secondary hair follicle-derived dermal papilla cells of the Cashmere goat (*Capra hircus*), *Physiol. Genom.* 46 (3) (2014) 104–111.
- [80] A. Hassan, D. Elebeedy, E.R. Matar, A.F.M. Elsayed, A.I. Abd El Maksoud, Investigation of angiogenesis and wound healing potential mechanisms of zinc oxide nanorods, *Front. Pharmacol.* 12 (2021).
- [81] H. Zhang, W. Ma, H. Ma, C. Qin, J. Chen, C. Wu, Spindle-like zinc silicate nanoparticles accelerating innervated and vascularized skin burn wound healing, *Adv. Healthc. Mater.* 11 (10) (2022) 2102359.
- [82] L. Shahzadi, A.A. Chaudhry, A.R. Aleem, M.H. Malik, K. Ijaz, H. Akhtar, F. Alvi, F. Khan, I.U. Rehman, M. Yar, Development of K-doped ZnO nanoparticles encapsulated crosslinked chitosan based new membranes to stimulate angiogenesis in tissue engineered skin grafts, *Int. J. Biol. Macromol.* 120 (2018) 721–728.